Description of a Cranial Endocast From the Fossil Mammal *Vincelestes neuquenianus* (Theriiformes) and Its Relevance to the Evolution of Endocranial Characters in Therians

THOMAS E. MACRINI,[1]* GUILLERMO W. ROUGIER,[2] AND TIMOTHY ROWE[1]
[1]Jackson School of Geosciences, The University of Texas at Austin, Austin, Texas
[2]Department of Anatomical Sciences and Neurobiology, School of Medicine, University of Louisville, Louisville, Kentucky

ABSTRACT

We generated a digital cranial endocast (infilling of the braincase) of *Vincelestes neuquenianus*, a Cretaceous theriiform mammal from Argentina, to achieve two goals. First, we described this endocast of *Vincelestes* to reconstruct the brain, associated soft-tissue structures, and internal osteological features. This report represents the first description of an endocast from a stem therian that is near crown group Theria (marsupials, placentals, and all descendants of that ancestor). Second, we examined 21 morphological characters related to the morphology of endocasts and endocranial osteology across 19 taxa (including *Vincelestes*) in the context of a current hypothesis about mammal phylogeny to identify potential synapomorphies for Theria. The digital endocast of *Vincelestes* is mostly complete, facilitating description in all views and allowing collection of accurate linear and volumetric measurements. However, it is unclear if the midbrain is exposed on the dorsal surface of the brain because of damage to this region of the endocast. Other portions of this specimen are extraordinarily well preserved, allowing identification of the accessory olfactory bulbs on the endocast, an ossified falx cerebri, and an osseous tentorium. The encephalization quotient (EQ) calculated for *Vincelestes* falls within the range of EQs of crown therians. Comparison of the endocranial characters across different mammalian taxa did not reveal any new synapomorphies for the clade Theria. Anat Rec, 290:875–892, 2007. © 2007 Wiley-Liss, Inc.

Key words: computed tomography; encephalization quotient; Mammalia; fossil; paleoneurology; brain evolution

There are over 5,400 species of extant mammals (Wilson and Reeder, 2005) that belong to two major clades, Theria and Monotremata (Fig. 1). Mammals are members of the clade Mammalia, which was defined phylogenetically as including the most recent common ancestor (hereafter "MRCA") between extant therians and extant monotremes, and all descendants of that ancestor (Rowe, 1988). Monotremata consists of the MRCA of all extant monotremes (four species of echidnas and the duckbill platypus; Wilson and Reeder, 2005) and all descendants of that ancestor. Theria contains the remaining overwhelming majority of extant mammalian species (5,412 therian species vs. 5 monotreme species;

Grant sponsor: National Science Foundation; Grant numbers: IIS 0208675, DEB 0309369 and DEB 0129061; Grant sponsor: Antorchas Foundation, Paleontological Exploration of Patagonia.

Dr. Macrini's current address is American Museum of Natural History, Department of Mammalogy, New York, NY 10024.

*Correspondence to: Thomas E. Macrini, American Museum of Natural History, Department of Mammalogy, Central Park West at 79th Street, New York, NY 10024. Fax: 212-769-5239. E-mail: tmacrini@amnh.org

Received 7 June 2006; Accepted 21 March 2007

DOI 10.1002/ar.20551

Published online 15 May 2007 in Wiley InterScience (www.interscience.wiley.com).

© 2007 WILEY-LISS, INC.

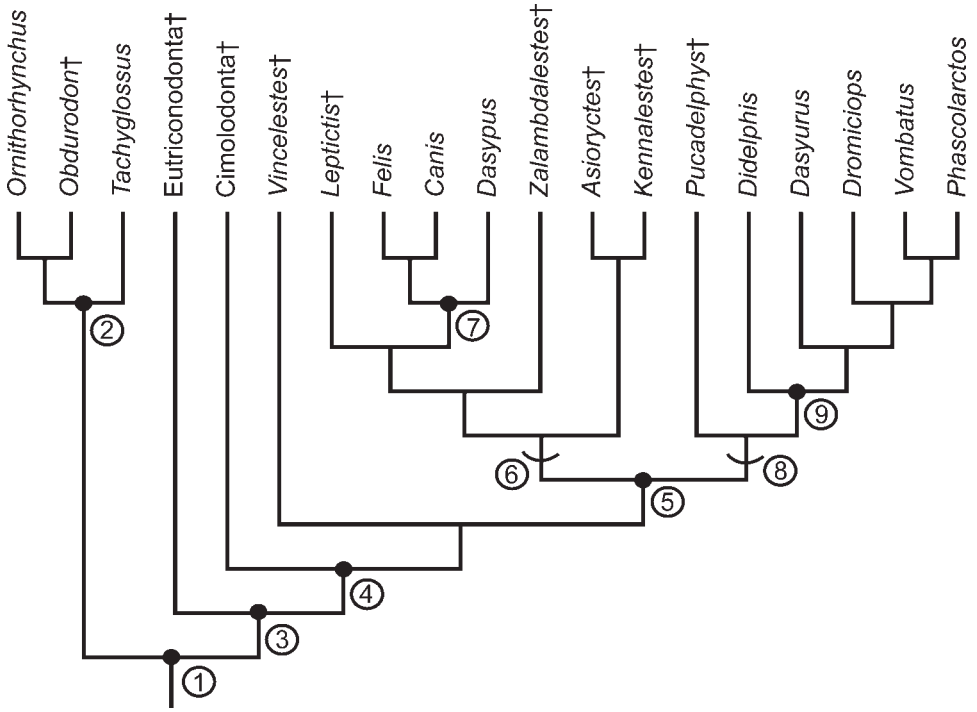

Fig. 1. Cladogram showing mammalian relationships based on a pruned strict consensus tree of Luo and Wible (2005). 1 = Mammalia (Rowe, 1988); 2 = Monotremata; 3 = Theriimorpha (Rowe, 1993); 4 = Theriiformes (Rowe, 1993); 5 = Theria; 6 = Eutheria (stem-based definition); 7 = Placentalia; 8 = Metatheria (stem-based definition; Rougier et al., 1998; Flynn and Wyss, 1999); 9 = Marsupialia (Rougier et al., 1998; Flynn and Wyss, 1999). Cimolodonta† is a clade within Multituberculata† (Kielan-Jaworowska et al., 2004). Daggers denote extinct taxon.

Wilson and Reeder, 2005) and is defined as comprising the MRCA between marsupials and placentals and all descendants of that ancestor (Rowe, 1988; Rougier et al., 1998). Thus, in this study, Mammalia, Monotremata, and Theria are all treated as crown groups (following Rowe, 1988), that is, taxa that comprise the MRCA of all extant members of a particular group, and all descendants of that ancestor (de Queiroz and Gauthier, 1990). Several fossil taxa are members of Mammalia but are excluded from Theria and Monotremata. These fossils are called stem taxa ("stem species" of Ax, 1985), because they lie along the branch leading to a crown group, but are excluded from that crown group. For example, stem therians are those fossil mammals that are more closely related to Theria than to Monotremata, but are not members of either crown group. We use the name "nonmammalian cynodonts" to refer to a paraphyletic group of extinct taxa that are closely related to crown mammals. Nonmammalian cynodont is the preferred term here because this is a more specific name than "stem mammal," which refers to a member of a much larger group of extinct taxa (i.e., nonmammalian synapsids).

Most stem therians are known from only fragmentary fossil remains and only a few of these taxa are represented by well preserved, undistorted cranial material (Kielan-Jaworowska et al., 2004). Because of this cranial endocasts (or representations of the space within the endocranial cavity) have only been studied in two stem therian groups, the eutriconodontans and the multituberculates (Simpson, 1927; Kielan-Jaworowska, 1983, 1984, 1986; Kielan-Jaworowska and Lancaster, 2004; Kielan-Jaworowska et al., 2004). Eutriconodontans are a group of mouse- to capybara-sized, animalivorous mammals that are known from the Mesozoic record of North America, South America, Europe, Africa, and Asia; they are characterized by molars with three main anteroposteriorly aligned cusps (Kielan-Jaworowska et al., 2004). Multituberculates are a speciose group of extinct mammals named for their multicusped molars and are represented by an extremely rich fossil record from the Mesozoic and early Tertiary of North America, South America, Europe, Africa, and Asia (Kielan-Jaworowska et al., 2004). One hypothesis of the placement of eutriconodontans and multituberculates along the therian stem is shown in Figure 1 (Luo and Wible, 2005). Based on this hypothesis, multituberculates are more closely related to Theria than eutriconodontans. An alternative hypothesis suggests that eutriconodontans are more closely related to Theria than multituberculates (Rougier et al., 1996; Wang et al., 2001; Kielan-Jaworowska et al., 2004). Following the former hypothesis, Theriiformes is defined as the clade containing the MRCA between multituberculates and therians and all descendants of that ancestor (Fig. 1; Rowe, 1993). Theriimorpha is a more inclusive group, which contains Theriiformes and eutriconodontans and all descendants of their MRCA (Fig. 1; Rowe, 1993).

An important stem therian is *Vincelestes neuquenianus*, a taxon from the Early Cretaceous of Argentina

(Bonaparte, 1986; Bonaparte and Rougier, 1987; Rougier et al., 1992). *Vincelestes* is one the most completely known stem therians, represented by six nearly complete skulls, 17 lower jaws, and several postcranial elements, all from a single quarry (Rougier et al., 1992; Rougier, 1993). Phylogenetic analyses incorporating relatively complete taxa place *Vincelestes* within the clade Theriiformes as the sister taxon to Theria (Fig. 1; Rougier, 1993; Rowe, 1993; Rougier et al., 1996). Analyses that include additional taxa of varying completeness of known skeletal material suggest that *Vincelestes* is more removed from Theria than some of the more incomplete taxa as a result of the relatively plesiomorphic dentition of *Vincelestes* (Rougier et al., 1998, 2004; Luo et al., 2002, 2003; Luo and Wible, 2005). However, these taxa, which are closer to Theria than *Vincelestes* are known from only very incomplete craniodental and skeletal fossils (Kielan-Jaworowska et al., 2004). Given the incomplete nature of these other stem therians, *Vincelestes* is operationally treated as the outgroup for Theria for studies that focus on cranial and postcranial character systems, and analyses restricted to the consideration of relatively complete taxa (Rowe, 1993; Rougier et al., 1996, 1998, 2004; Novacek et al., 1997; Horovitz, 2000, 2003; Wible et al., 2001; Horovitz and Sánchez-Villagra, 2003).

The skull of *Vincelestes* (Fig. 2) is well-studied and is useful for determining homologies of problematic cranial features and for determining the polarity of cranial characters in the MRCA of therians, particularly in relation to the sidewall of the braincase (Rougier et al., 1992; Hopson and Rougier, 1993; Rougier and Wible, 2006), the petrosal (Rougier et al., 1992; Wible and Hopson, 1993), and the cranial vasculature pattern (Rougier et al., 1992). Although the exterior of the skull of *Vincelestes* is well described in the literature (Bonaparte and Rougier, 1987; Rougier et al., 1992; Hopson and Rougier, 1993), the internal cranial osteology and cavities within the skull are virtually unknown, except those described in association with an isolated petrosal (Rougier et al., 1992, 1996). No natural cranial endocasts are known for *Vincelestes*.

A cranial endocast (sensu Colbert et al., 2005; Macrini et al., 2006, 2007) is a three-dimensional representation of the space within the endocranial cavity of the skull. The endocranial cavity of mammals comprises the confluent ethmoidal fossa for the olfactory bulbs, and the cerebral and cerebellar cavities. The brain fills most of this space in the majority of mammals, leaving an impression on the internal surfaces of the braincase bones in many taxa (Jerison, 1973). This fact allows the opportunity to study the brains of extinct mammals through examination of cranial endocasts (e.g., Marsh, 1884; Simpson, 1927; Edinger, 1948; Jerison, 1973; Radinsky, 1977, 1978, 1981; Kielan-Jaworowska, 1984, 1986).

In addition to the brain, other soft tissue may leave an impression on the endocast and partially obscure the morphology of the brain. Mammals have three connective tissue sheets called meninges (dura mater, arachnoid, pia mater) that surround and cushion the brain (Butler and Hodos, 1996). In places, particularly along the ventral aspect of the brain, the meninges are separated, resulting in spaces between these layers. These spaces are filled by cerebrospinal fluid (CSF) and particularly expansive subarachnoid spaces are called cisterns (Evans, 1993; Butler and Hodos, 1996). Dural sinuses (e.g., superior sagittal sinus, transverse sinus, sigmoid sinus, prootic sinus) are segments of the venous system located within the dura mater (Butler, 1967; Kielan-Jaworowska et al., 1986; Evans, 1993). Cranial nerves are the nerves that emerge from the brain; mammals and amniotes in general have 12 pairs that are denoted by Roman numerals (cranial nerves I–XII), although some count additional nerves among these, such as the terminal nerve (nerve 0; Butler and Hodos, 1996).

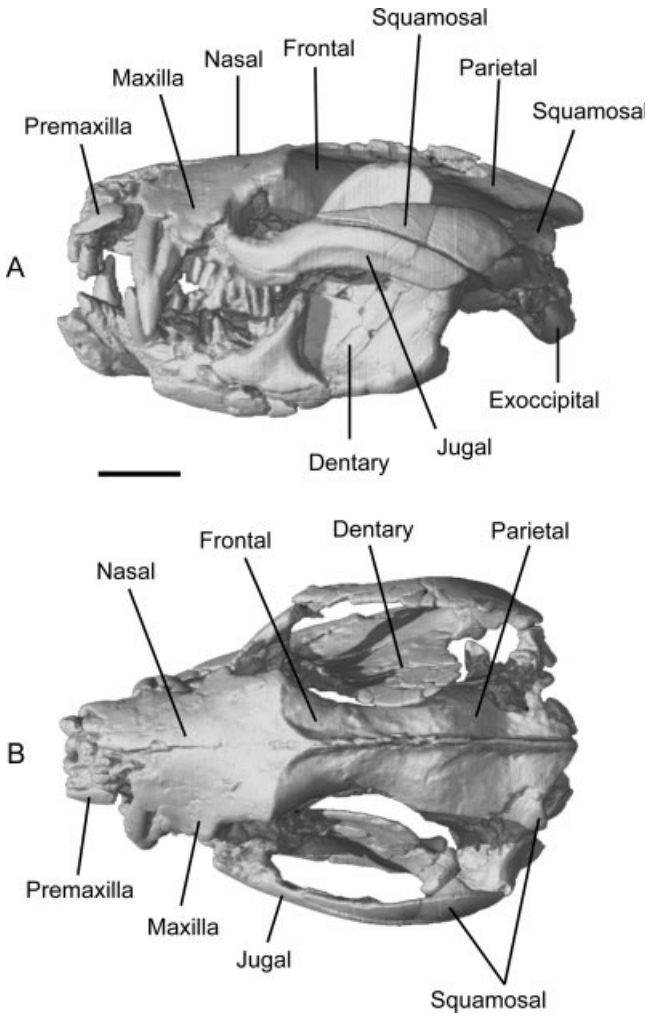

Fig. 2. Digital rendering of the skull of *Vincelestes neuquenianus* (MACN-N 04) in two views. **A:** Left lateral view. **B:** Dorsal view. Scale bar = 1 cm.

Intervention of the structures listed above prevents some major external features of the brain from leaving impressions on the internal surfaces of surrounding bones and from being represented on cranial endocasts (Bauchot and Stephan, 1967; Jerison, 1973). The degree of representation of external brain features on endocasts varies taxonomically among mammals. But, in general, a great amount of brain morphology is visible on the corresponding endocasts of many extant mammalian taxa, facilitating comparisons of gross neuroanatomy between

extinct and extant taxa (e.g., Edinger, 1948; Bauchot and Stephan, 1967; Radinsky, 1968, 1973, 1975; Jerison, 1973; Lyras and van der Geer, 2003; Macrini et al., 2006, 2007).

For this study, a cranial endocast was extracted by means of computed tomography (CT) scans of a single skull of *Vincelestes* and analyzed to achieve two goals. First, we describe this endocast to reconstruct the brain, associated soft-tissue structures, and internal cranial osteological features of *Vincelestes*. Second, we compare aspects of the morphology of the endocast and endocranial osteology of *Vincelestes* to those of other crown mammals. These endocranial characters are examined in the context of a current hypothesis about the phylogenetic relationships of mammals (Fig. 1) with the purpose of reconstructing character states for the MRCA of crown therians to identify potential synapomorphies for Theria.

MATERIALS AND METHODS

Specimen Examined

A digital endocast was extracted from a skull of *Vincelestes neuquenianus* (MACN-N 04) from the collections of the Museo Argentino de Ciencias Naturales in Buenos Aires, Argentina. The specimen was collected from the Lower Cretaceous La Amarga Formation (Legarreta and Uliana, 1999) of southern Neuquén Province, Argentina. This skull is mostly complete (Hopson and Rougier, 1993), and there is little apparent distortion or plastic deformation to the braincase bones of this skull (i.e., these bones are not warped). Accordingly, the corresponding endocast is relatively undistorted; however, there is moderate to heavy damage to some portions of the skull, probably due to weathering or predepositional transport. Specifically, the rostrum and right side of the braincase (Fig. 2), particularly the right petrosal, are damaged, as are the internal surfaces of some of the braincase bones. Moderate damage to external and internal surfaces of the lateral braincase bones (parietal, alisphenoid, anterior lamina of the petrosal, squamosal) on the left side of the skull is also evident. Delicate internal bony structures such as the ossified falx cerebri and cribriform plate are broken or poorly preserved, affecting the representation of some anatomical features on the endocast such as casts of dural sinuses and the anterior portion of the olfactory bulb casts.

This skull of *Vincelestes* (MACN-N 04) measures 63.00 mm from the anterior tip of the premaxillae to the back of the occiput and is likely from an old adult based on tooth wear (Rougier, 1993). There is possible sexual dimorphism among the known adult skulls of *Vincelestes*, and because this specimen belongs to the smaller of the two size classes, it is presumably a female (Rougier, 1993).

A body mass estimate was obtained for MACN-N 04 using the following equation relating body weight and skull length in extant insectivorans: $y = 3.68x - 3.83$. In this equation, $y = \log_{10}$(body weight) in g, and $x = \log_{10}$(skull length) in millimeters (Luo et al., 2001, Fig. 5B). Note that the use of $\log_{10}$ and not Ln for this equation is correct according to Luo (personal communication).

The body mass of the specimen of *Vincelestes* examined in this study is estimated at 619 g. However, the maximum size range for *Vincelestes* is considerably larger (900 to 1,228 g). The 900 g estimate was determined by Rougier (1993) based on the largest isolated humeri and femora and using the formulae of Alexander et al. (1979). The 1228 g estimate was determined from the largest known skull of *Vincelestes* using the modified equation from Luo et al. (2001). However, *Vincelestes* is near the upper range of size for extant insectivorans and a formula based on a sample of larger extant mammals might be more appropriate for estimating the maximum body mass for *Vincelestes*.

TABLE 1. Relevant Web addresses

Description	Web address
UTCT Web site	<www.ctlab.geo.utexas.edu/index.php>
Digimorph homepage	<www.digimorph.org>
Vincelestes CT movies	<www.digimorph.org/specimens/Vincelestes_neuquenianus>
Didelphis CT movies	<www.digimorph.org/specimens/Didelphis_virginiana>
Wallabia CT movies	<www.digimorph.org/specimens/Wallabia_bicolor>

CT Scanning

The skull of *Vincelestes* was CT scanned at the University of Texas High-Resolution X-ray Computed Tomography Facility in Austin, Texas (UTCT). Detailed descriptions of high resolution CT and its capabilities for imaging vertebrate cranial osteology are published elsewhere (e.g., Rowe et al., 1995; Denison et al., 1997; UTCT Web site, see Table 1). The skull of *Vincelestes* was scanned in its entirety in the coronal (i.e., transverse of some authors) slice plane from front to back. The scanning resulted in 315 slices (i.e., images) with dimensions of 512×512 pixels. The slices are 0.21 mm thick with an interslice spacing (the space between consecutive slices) of 0.20 mm, resulting in a slice overlap of 0.01 mm. Two-dimensional slices were reconstructed from X-rays using a field of reconstruction value of 49 mm, a reconstruction offset of 0, and a reconstruction scale of 38.

Extraction of Endocast

A digital endocast was extracted from the CT scans of the skull of *Vincelestes* using the program VGStudioMax© (version 1.2; Volume Graphics GmbH, 2004) and following procedures described in the literature (Macrini et al., 2006, 2007). VGStudioMax© was also used to segment portions of the endocast, representing distinct structures such as the olfactory bulb casts, parafloccular casts, and hypophyseal fossa casts. The boundaries of these structures were determined following protocols described in previous papers (Macrini et al., 2006, 2007).

We also used VGStudioMax© to calculate volumes and partial volumes, to take linear measurements of the extracted endocast segments, and to generate movie frames of the rotating endocasts. Endocast flexure was measured following the procedure described and illustrated in Macrini et al. (2007). A list of measurements from *Vincelestes* is presented in Table 2.

TABLE 2. Endocast measurements for *Vincelestes neuquenianus* (MACN-N 04)

Endocast flexure[a]	23°
Endocranial volume[b]	2371.215 mm^3
Endocast anteroposterior length[b]	31.800 mm
Endocast maximum width	17.514 mm
Endocast maximum height	10.721 mm
Olfactory bulb cast volume[c]	256.238 mm^3
Olfactory bulb cast anteroposterior length	9.200 mm
Olfactory bulb cast maximum width[c]	9.092 mm
Olfactory bulb cast maximum height	6.348 mm
Left cerebral hemisphere cast diagonal length[d]	13.500 mm
Left cerebral hemisphere cast maximum width[d]	6.000 mm
Left cerebral cast maximum height[e]	8.000 mm
Hypophyseal cast volume	16.935 mm^3
Hypophyseal cast anteroposterior length	4.211 mm
Hypophyseal cast maximum width	4.200 mm
Hypophyseal cast maximum height	2.584 mm
Parafloccular cast volume[f]	5.365 mm^3
Vermis cast anteroposterior length[g]	5.500 mm
Vermis cast maximum width[g]	6.500 mm

[a]Measured following procedure of Macrini et al. (2007).
[b]Value includes olfactory bulb casts.
[c]Combined value for bilateral structures.
[d]Length measured along long axis of cerebral hemisphere cast in dorsal view; width measured perpendicular to long axis.
[e]Measured in lateral view.
[f]Volume of left parafloccular cast only.
[g]Measured in dorsal view.

VGStudioMax© provides measurements with accuracy to the third decimal place (i.e., 0.001). Measurements are given verbatim from VGStudioMax© to a thousandth of a millimeter (micron); however, it is uncertain if the actual measurements are accurate to that level. Linear measurements are presented from the left cerebral hemisphere only; measurements from the right cast are nearly identical.

Surface models of the endocasts were generated using VGStudioMax© and then exported to Amira 3.1™ (Zuse Institute Berlin, 2004) where the surfaces of the endocasts were smoothed. Rotation movies of the smoothed digital endocast were compiled and are available for viewing on the Digimorph Web site (Table 1). Images of the smoothed endocasts are used in the figures of this study, but volumetric measurements were obtained before smoothing the endocasts. Anatomical features were identified before smoothing the endocasts even though it is unlikely that the process of smoothing would erase a major feature such as a sulcus.

In the description of the endocast of *Vincelestes*, we make comparisons with endocasts or skulls of extant mammals such as *Didelphis virginiana*, the Virginia opossum (TMM M-2517; Macrini, 2006; Macrini et al., 2007), and *Wallabia bicolor*, the swamp wallaby (TMM M-4169), both from the Texas Natural Science Center extant mammal collections housed at the Vertebrate Paleontology Laboratory in Austin, Texas. We also make comparisons with published descriptions of digital endocasts, natural endocasts, and brains from various other crown mammals. Specific CT images of the skull of *Vincelestes* are cited in the description in reference to anatomical structures; these images are visible on the Web (Table 1). The prefix 'C' is used to designate the coronal plane and 'S' designates the sagittal plane. Consecutive CT images are rendered with a dash (e.g., C100-102).

Phylogenetic Character Matrix

The second goal of this study is to examine phylogenetic characters pertaining to endocasts and endocranial osteology using data from the endocast of *Vincelestes* and other endocasts of crown mammals. To address this goal, we examined the distributions of 21 endocranial characters on a pruned version of the strict consensus tree topology (Fig. 1) obtained from a phylogenetic analysis by Luo and Wible (2005). Characters were traced on the tree topology using parsimony ancestral state reconstruction in Mesquite (version 1.12; Maddison and Maddison, 2006).

Quantitative data were converted to discrete characters (e.g., characters 1, 15, 17, 18) based on the distribution of the observed data. However, the assignment of these data into discrete bins is somewhat arbitrary. We realize that conversion of quantitative data to discrete characters might not be optimal for inferring phylogenetic relationships, and instead, treatment of these data as continuous characters is preferred by some (papers in MacLeod and Forey, 2002). We provide references for the sources of the quantitative data for every taxon we examined in this study (Table 3), in case subsequent workers choose to treat these data as continuous characters in phylogenetic analyses.

DESCRIPTION

The endocast of *Vincelestes* in dorsal view has the approximate shape of two cylinders: a small anterior one consisting of the two olfactory bulb casts and a larger posterior one comprising the rest of the endocast (Fig. 3). The width/length aspect ratio of the endocast is 0.55, the height/length ratio is 0.34, and the height/width ratio is 0.61. All linear and volumetric measurements from the endocast are presented in Table 2.

The lateral profile of the endocast reveals that the center of the dorsal surface of the cerebral hemisphere cast is humpbacked; the dorsal surface slopes up from the posterior of the endocast and then anteriorly it slopes down before the circular fissure (Fig. 3A,A′). Posterior to the dorsal hump, there is a shallow concavity on the dorsal profile of the endocast in the midbrain region (Fig. 3A). Posterior to the concavity is another dorsal convexity representing the dorsal surface of the cast of the vermis of the cerebellum (Fig. 3B,B′). The endocast dorsal surface slopes down severely posterior to the vermis cast and then levels out at the foramen magnum (Fig. 3B,B′).

Forebrain Region of Endocast

The olfactory bulb casts are the anteriormost structures on the forebrain cast of *Vincelestes*. These casts represent the space occupied by the main olfactory bulbs and associated meninges. The shapes of the casts are of prominent, anteroposteriorly elongated ovoids with a width/length aspect ratio of 0.49 (Fig. 3). Together, the two casts constitute 10.81% of the total endocranial cavity.

TABLE 3. Taxon–endocranial character matrix[a]

Taxon	1	2	3	4	5	6	7	8	9	10	11	12	13	14	15	16	17	18	19	20	21
Ornithorhynchus	1	0	0	1	0	1	1	0	1	0	0	1	1	0	0	1	1	1	0	0	1
Obdurodon†	1	0	0	?	0	1	1	0	1	0	0	1	1	0	0	1	1	1	0	0	0
Tachyglossus	?	0	0	0	1	1	N	1	0	0	0	N	1	1	N	N	1	1	0	1	0
Eutriconodonta†	0	0	?	1	0	?	0	0	?	?	0	0	?	0	?	1	?	?	?	1	?
Cimolodonta†	1	0	0	1	0	0	0	1	?	?	0	0	0	0	1	2	0	0	0	0	?
Vincelestes†	0	1	?	1	0	0	0	0	1	1	?	0	1	0	0	0	2	2	1	1	1
Asioryctes†	0	0	?	1	0	?	?	0	?	?	1	?	?	0	?	?	?	?	?	1	?
Kennalestes†	0	1	?	?	0	0	?	0	?	?	1	?	?	0	?	?	?	?	?	1	?
Zalambdalestes†	0	0	?	1	0	?	1	0	?	?	1	1	?	0	?	1	?	?	?	1	?
Leptictis†	0	0	?	1	1	1	0	1	?	?	0	1	1	0	?	1	?	0	?	1	0
Canis	0	0	0	1	1	1	1	1	0	1	0	1	0	0	0	3	1	0	0	1	0
Felis	1	0	0	1	1	1	N	1	0	3	0	N	1	1	N	N	2	2	0	1	0
Dasypus	0	0	0	1	1	1	N	1	0	0	0	N	1	1	N	N	2	2	0	1	0
Pucadelphys†	0	0	?	1	0	0	0	0	0	0	0	0	1	0	0	1	0	0	?	1	0
Didelphis	0	0	1	1	0	1	1	1	0	0	0	1	1	0	0	3	1	1	0	1	0
Dromiciops	1	0	0	1	0	1	1	1	0	0	0	1	1	0	1	1	1	1	1	1	0
Dasyurus	0	0	0	1	0	1	0	1	0	0	0	1	1	0	1	1	1	1	0	1	0
Vombatus	1	0	0	0	1	1	N	1	0	0	0	N	1	1	N	N	1	1	1	1	0
Phascolarctos	1	0	0	0	0	1	0	0	0	0	0	0	1	0	0	3	1	1	1	1	0

[a]Character data sources: *Ornithorhynchus andinus*, *Obdurodon dicksoni*†, *Tachyglossus aculeatus* (Macrini et al., 2006); Eutriconodonta† (*Priacodon fruitaensis*† [Rougier et al., 1996], *Triconodon mordax*†, *Triconodon ferox*† [Simpson, 1927; Kermack, 1963]); Cimolodonta† (*Chulsanbaatar vulgaris*† [Kielan-Jaworowska, 1983, 1986], *Kryptobaatar dashzevegi*† [Kielan-Jaworowska and Lancaster, 2004], *Nemegtbaatar gobiensis*† [Kielan-Jaworowska, 1986], *Ptilodus montanus*† [Krause and Kielan-Jaworowska, 1993]); *Vincelestes neuquenianus*† (Rougier et al., 1992; this paper); *Asioryctes nemegetensis*†, *Zalambdalestes lechei*†, *Kennalestes gobiensis*† (Kielan-Jaworowska, 1984, 1986; Wible et al., 2004); *Leptictis dakotensis*† (Novacek, 1982, 1986); *Canis lupus*, *Felis silvestris catus*, *Dasypus novemcinctus* (Macrini, 2006); *Pucadelphys andinus*†, *Didelphis virginiana*, *Dromiciops australis*, *Dasyurus hallucatus*, *Vombatus ursinus*, *Phascolarctos cinereus* (Marshall and Muizon, 1995; Sánchez-Villagra, 2002; Macrini et al., 2007). N, not applicable; ?, unknown data; †, extinct taxon.

Immediately posterior to each olfactory bulb cast is a crescent-shaped accessory olfactory bulb cast (Fig. 3). The olfactory and accessory olfactory bulb casts, together comprising the "olfactory bulb region," are separated from the rest of the endocast by a broad, flat circular fissure (Fig. 3; Loo, 1930; Rowe, 1996a,b; i.e., transverse furrow of Kielan-Jaworowska, 1986; transverse sulcus of Krause and Kielan-Jaworowska, 1993; circular sulcus of Luo et al., 2002). In dorsal and lateral views, the olfactory bulb region is separated from the rest of the endocast by a distinct neck (Fig. 3), a portion of the endocast that incorporates the olfactory peduncle and surrounding cortex (Nieuwenhuys et al., 1998). A similar "neck" is visible in the lateral view of the brain of *Didelphis virginiana* (Loo, 1930). The olfactory tracts leading from the olfactory bulbs to the cortex did not leave an impression on the ventral surface of the endocast of *Vincelestes*.

The cerebral hemisphere casts are immediately posterior to the circular fissure. In the dorsal view, the cerebral hemisphere casts are anteroposteriorly elongated ovoids (Fig. 3B,B′) with lissencephalic surfaces, that is, smooth and lacking gyri and sulci. Gyri are ridges of cerebral cortex and sulci are the troughs between the gyri (Butler and Hodos, 1996). The width/length aspect ratio of the left cerebral hemisphere cast is 0.44. The hemisphere casts are divided medially by a deep median sulcus (Fig. 3B,B′) at their anterior end; a result of the presence of an ossified falx cerebri, which occupies this space between the casts (Fig. 4). Posteriorly, the casts diverge from each other and the endocast midline, separating around the cast of the vermis of the cerebellum (Fig. 3B,B′). This finding is similar to the condition seen in the endocasts of multituberculates as exemplified by *Kryptobaatar dashzevegi* (Kielan-Jaworowska and Lancaster, 2004).

The posteromedial edges of each cerebral hemisphere cast of *Vincelestes* are damaged because the ossified falx cerebri is broken (Fig. 4), leaving a large depression on the dorsoposterior surface of the endocast (Fig. 3B). The depression has the shape of a "T" with the top portion of the "T" abutting the anterior edge of the vermis cast (Fig. 3B).

The cerebral hemisphere casts appear as ovoids in lateral view; the left cast has a height/length aspect ratio of 0.59. There is a broad roughened area on the lateral surface of the left cerebral hemisphere cast (Fig. 3A), a result of damage to the portions of the parietal, alisphenoid, and anterior lamina of petrosal that contribute to the braincase wall of this skull of *Vincelestes*. This is in the area where a rhinal fissure would be expected. The right side of the endocast is better preserved and reveals that a fissure is not present on the lateral surface of the endocast (refer to CT movies on Web, Table 1).

The posterior portion of the superior sagittal sinus (sss) of *Vincelestes* was transmitted through a bony canal with a subcircular cross-section (C225-241) that is located within the dorsal portion of the ossified falx cerebri. Because the canal is surrounded by bone, the sss does not leave an impression on the dorsal surface of the endocast of *Vincelestes*.

Midbrain Region of Endocast

The endocranial surface of the skull is damaged in the region corresponding to the midbrain of the endocast. Because of this damage, it is impossible to determine

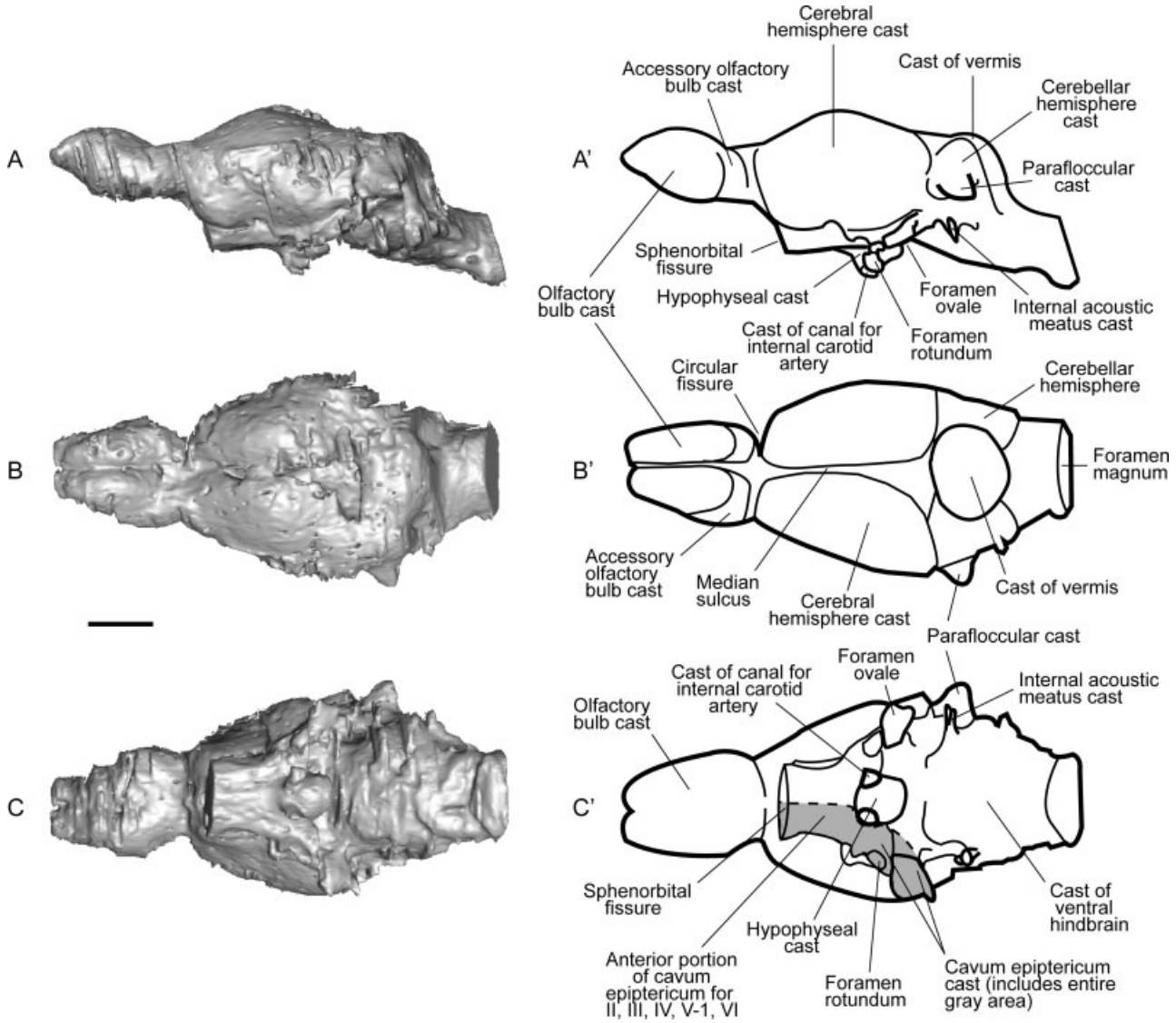

Fig. 3. Digital rendering of the cranial endocast of *Vincelestes neuquenianus* (MACN-N 04) in three views. **A:** Left lateral view. **B:** Dorsal view. **C:** Ventral view. Line drawings of the cranial endocast with anatomical labels in three views. **A′:** Left lateral view. **B′:** Dorsal view. **C′:** Ventral view. Foramen ovale transmitted cranial nerve V_3; foramen rotundum transmitted cranial nerve V_2; internal acoustic meatus transmitted cranial nerves VII and VIII; sphenorbital fissure transmitted cranial nerves II, III, IV, V_1, and VI. Scale bar = 5 mm.

whether the superior and inferior colliculi leave their mark on the dorsal surface of the endocast of *Vincelestes*. Transverse sinus casts are also expected to be in this region of the endocast, but are not visible because of this damage. It is uncertain if these sinus casts cover the dorsal exposure of the midbrain in *Vincelestes* as occurs in endocasts of many fossil and extant mammals (e.g., *Tenrec ecaudatus*, Bauchot and Stephan, 1967; *Monodelphis domestica*, the gray short-tailed opossum; Macrini et al., 2007).

Hindbrain Region of Endocast

Fragments of a broken osseous tentorium are visible on the CT images of *Vincelestes* (C254-264; S105-124) directly posterior to the ossified falx cerebri. This structure provides a dorsal division between the cerebellar cavity and the cerebral cavity of the braincase. The osseous tentorium of *Vincelestes* has the shape of a dorsoventrally compressed diamond in coronal cross-section (Fig. 5), and the overall shape is reminiscent of the same structure of the macropodid marsupials *Macropus* and *Wallabia*.

Casts of the vermis and cerebellar hemispheres are clearly visible on the endocast of *Vincelestes* (Fig. 3). The vermis cast is roughly semispherical in shape when viewed dorsally (Fig. 3B,B′); the width/length aspect ratio is 1.18, indicating that the vermis cast is slightly wider than long. However, the extreme anterior edge of the cast is not discernable due to the depression on the

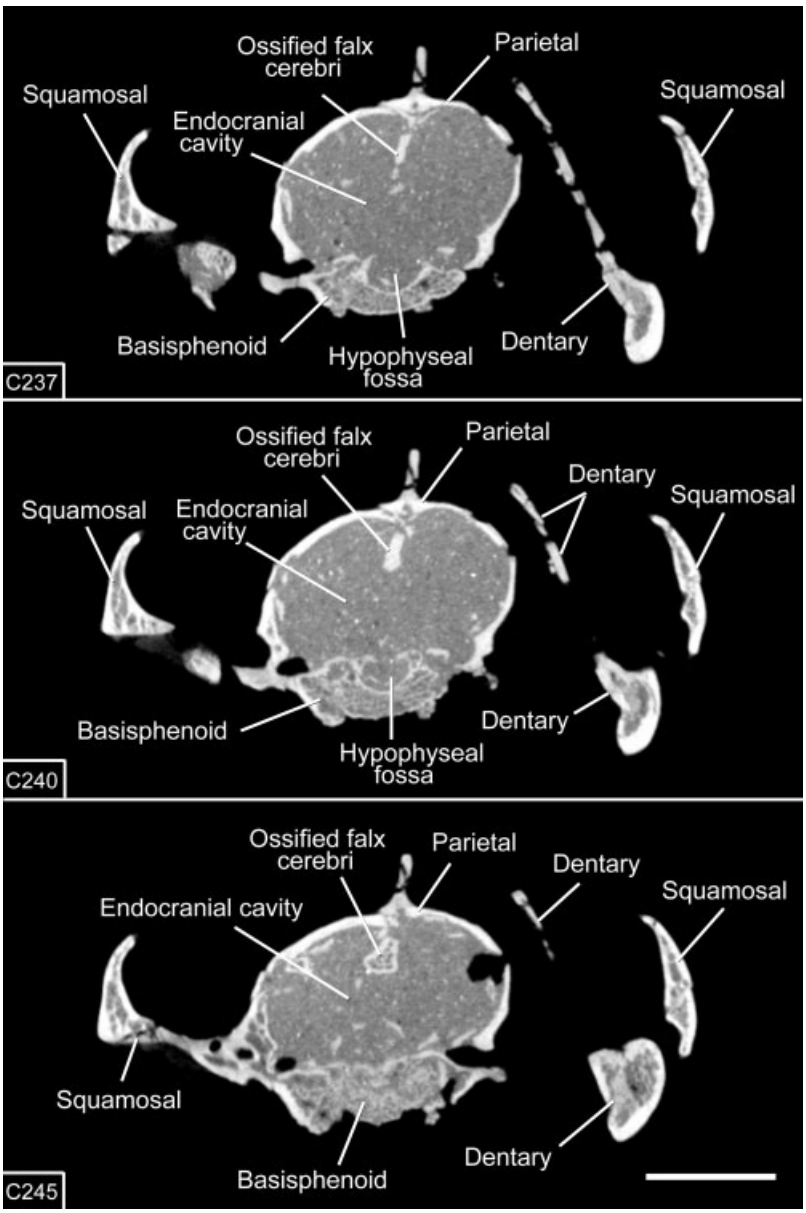

Fig. 4. Coronal computed tomographic images through the braincase of *Vincelestes neuquenianus* (MACN-N 04) showing the ossified falx cerebri. The slice number is indicated in lower left hand corner of each image; C237 is the anteriormost image. Scale bar = 1 cm (all three images are at the same scale).

endocast caused by the broken ossified falx cerebri (Fig. 3). Even so, it is clear that the vermis cast extends anterior to the position of the parafloccular cast (Fig. 3B,B′).

The cerebellar hemisphere casts are not well separated from the rest of the cast of the cerebellum but they are clearly present on the endocast of *Vincelestes* (Fig. 3B,B′), unlike the endocasts of multituberculates, which lack cerebellar hemispheres (Kielan-Jaworowska, 1983, 1986; Kielan-Jaworowska and Lancaster, 2004). A conical cast of the paraflocculus extends laterally from the left cerebellar hemisphere cast (Fig. 3). This structure on the endocast corresponds with the subarcuate fossa of the petrosal bone, which was described by Rougier et al. (1992) as a "cone-shaped hollow." The subarcuate fossa of *Vincelestes* and the corresponding parafloccular cast differ from the deep, subspherical morphology of the fossae and parafloccular casts seen in basal metatherians (Wible, 1990; Rougier et al., 1998) and basal eutherians (MacIntyre, 1972; Kielan-Jaworowska, 1984, 1986; Meng and Fox, 1995; Wible et al., 2001, 2004; Ekdale et al., 2004). The subarcuate fossa of the right petrosal of the skull of MACN-N 04 is damaged, preventing the representation of a parafloccular cast on the right side of the endocast.

The cast of the internal acoustic meatus (IAM) is located ventral and somewhat anterior to the parafloccular cast

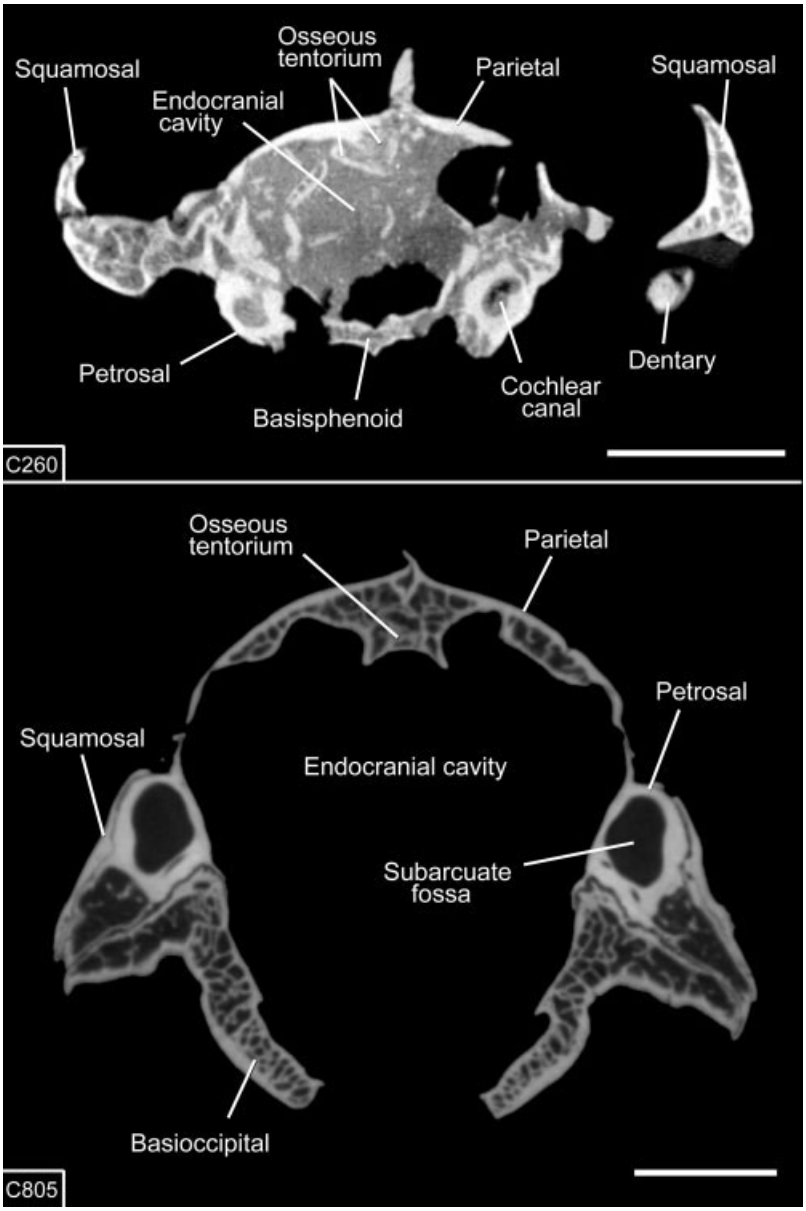

Fig. 5. Coronal computed tomographic images through the braincase of *Vincelestes neuquenianus* (MACN-N 04; top image), and *Wallabia bicolor* (TMM M-4169), the swamp wallaby (Macropodidae; bottom image) showing the osseous tentorium. The slice number is indicated in the lower left-hand corner of each image. Scale bars = 1 cm.

and is visible in lateral and ventral views of the endocast of *Vincelestes* (Fig. 3; Rougier et al., 1992). The IAM has the shape of a horizontally oriented "Y" with the thick base being medial and a lateral bifurcation for the thinner canals that transmitted cranial nerves VII and VIII (Fig. 3C,C′; C260-264, C267-271). The dorsal canal, which transmitted the facial nerve (VII), is more vertically directed than in the opossum, *Monodelphis domestica*, which has a more horizontally oriented canal. Similar to the description of an isolated petrosal of *Vincelestes* (MACN-N 16; Rougier et al., 1992), the specific foramina inside the IAM are not identifiable on these CT images of MACN-N 04.

The blood vessels that leave impressions on the petrosal of *Vincelestes* were reconstructed in detail elsewhere (Rougier et al., 1992), based on an isolated petrosal and additional cranial material. These structures are not described here for this specimen of *Vincelestes*, except to say that the cast of the prootic canal, which transmitted the prootic sinus (Rougier et al., 1992), is visible in the CT slices (C260-264), but is not visible on the endocast. The sigmoid sinus described elsewhere for *Vincelestes* (Rougier et al., 1992) cannot be identified on the CT images and the corresponding endocast because the portions of the anterior lamina of the petrosal, squamosal,

and parietal near the ear region are damaged on both sides of this skull of *Vincelestes*.

Little detail is discernable on the ventrum of the hindbrain cast in *Vincelestes*. The hindbrain cast is somewhat uneven in places due to damage on the internal surfaces of the basicranial bones. However, the medulla oblongata and the pons did not appear to leave distinctive impressions on the endocast (Fig. 3C,C′); these structures were likely obscured in ventral view by meninges and the pontine cistern as in other mammals (Evans, 1993).

Midventral Surface of the Endocast

The cast of the hypophyseal fossa is located in the center of the ventral surface of the endocast of *Vincelestes* (Fig. 3C,C′). The hypophyseal fossa of *Vincelestes* is a circular, deep, depression with a width/length aspect ratio of approximately 1.00, and a height/length ratio of 0.61. The cast of the hypophyseal fossa composes approximately 0.71% of the entire endocranial cavity.

A cast of the canal that transmitted the internal carotid artery converges on the anterolateral portion of each side of the hypophyseal cast in *Vincelestes* (Fig. 3C,C′). The foramen for the entrance of each internal carotid artery is oriented nearly vertical and is located ventrolateral to the anterior portion of the hypophyseal cast. This contrasts with the condition seen in an endocast of *Didelphis virginiana* in which each internal carotid artery canal enters the hypophyseal cast in a more posterolateral position and the internal carotid foramen is located posterolateral to the hypophyseal cast (figured in Macrini, 2006).

The cast of the cavum epiptercium is represented on the endocast as the crescent-shaped bulge from the sphenorbital fissure continuing posterior to the foramen ovale (Fig. 3C,C′). The right and left cava of *Vincelestes* are confluent for the anterior portion leading up to the sphenorbital fissure (Fig. 3C,C′); this space and the fissure presumably transmitted cranial nerves II, III, IV, V_1, and VI (Hopson and Rougier, 1993). The anterior portions of the right and left cava epipterica are also confluent on skulls and endocasts of *Ornithorhynchus anatinus*, the platypus (Zeller, 1989a; Macrini et al., 2006).

The posterior portion of the cavum epiptericum incorporates the space surrounding the foramen rotundum (for V_2) and foramen ovale (for V_3; Fig. 3C,C′). The geniculate ganglion of the facial nerve (VII) was located in the separate cavum supracochleare located within the petrosal, but connected to the cavum epiptericum by means of an opening termed the fenestra semilunaris (Rougier et al., 1992).

DISCUSSION

Endocranial Characters

Below is a list and description of characters pertaining to endocasts and endocranial osteology. The character matrix is provided in Table 3, and the distribution of character states among mammals is discussed below. We report all the characters we examined regardless of informativeness with the reasoning that the characters that are uninformative for our study might be informative when examined in a broader taxonomic context.

We do not include characters pertaining to the petrosal, except for those structures that are typically represented on the cranial endocasts (e.g., parafloccular cast representing subarcuate fossa of petrosal). Osteological characters of the petrosal pertaining to *Vincelestes* and other crown mammals are discussed in detail in the literature (e.g., MacIntyre, 1972; Rowe, 1988, 1993; Wible, 1990; Rougier et al., 1992, 1996, 1998, 2004; Meng and Fox, 1995; Wible et al., 2001; Luo et al., 2002, 2003; Ekdale et al., 2004; Luo and Wible, 2005; Rougier and Wible, 2006). However, we do include osteological characters pertaining to the endocranial cavity that are not typically incorporated in phylogenetic analyses (e.g., presence or absence of ossified falx cerebri).

Character 1. Percent of endocast composed of olfactory bulb casts: 6% or greater (large) (0), or less than 6% (small) (1). Based on the taxonomic sample we examined, 6% is the mean for this value. The casts of olfactory bulbs on endocasts provide a good approximation of the size and shape of the corresponding olfactory bulbs in extant mammals (Edinger, 1948; Bauchot and Stephan, 1967; Radinsky, 1968, 1973, 1975; Macrini et al., 2006), and olfactory bulb size is known to correlate with endoturbinal surface area and olfactory acuity in some extant mammals (e.g., Nieuwenhuys et al., 1998; Rowe et al., 2005). Therefore, this character has biological significance.

Olfactory bulb casts are large (in the sense mentioned above) in *Triconodon*, *Vincelestes*, and many of the therians examined in our sample. This finding suggests that the MRCA of therians and the MRCA of mammals had large olfactory bulbs. Reduction or complete loss of the olfactory bulbs occurs in the cetaceans and sirenians within Placentalia (e.g., Edinger, 1955; Jerison, 1973; Meisami and Bhatnagar, 1998; Marino, 2004; Colbert et al., 2005), and the aquatic platypus in Monotremata (Pirlot and Nelson, 1978; Macrini et al., 2006). These deviations from the primitive mammalian morphology were acquired convergently in those lineages and are presumably related to the reduced sense of smell in aquatic mammals (Negus, 1958; Pirlot and Nelson, 1978; Meisami and Bhatnagar, 1998).

Character 2. Accessory olfactory bulb casts: absent (0), or visible on endocast (1). Accessory olfactory bulbs of extant mammals receive projections from the vomeronasal organ, an organ that functions in the detection of pheromones (Nieuwenhuys et al., 1998). The accessory olfactory bulbs are not often represented on endocasts of extant mammals (e.g., Bauchot and Stephan, 1967; Jerison, 1973; Macrini et al., 2006, 2007). In our sample, casts of these structures are only seen on *Vincelestes*, and also reportedly on the eutherian *Kennalestes* (Kielan-Jaworowska, 1984).

Character 3. Olfactory bulb tracts: not visible on endocast (0), or visible on endocast (1). The olfactory tracts are the projections of the olfactory bulbs to the telencephalon (Butler and Hodos, 1996). Among the taxa we sampled, only *Didelphis* has olfactory bulb tracts represented on its endocast. The meninges and associated structures often obscure the visibility of olfactory bulb tracts on endocasts. The condition in *Vincelestes* is

unknown because there is damage to the bones underlying the ethmoidal fossa (cavity for the olfactory bulb) in the corresponding skull.

Character 4. Circular fissure: shallow or absent (0), or deep (1) on endocast. This character is modified from Luo and Wible (2005, character 418). The annular ridge of the frontal bone (Rowe et al., 2005; Macrini et al., 2007; "transverse ridge" of Nieuwenhuys et al., 1998:1642) is the bony element that sits in the circular fissure of the brain and separates the olfactory bulbs from the rest of the brain. Thus, the circular fissure marks the posterior extent of the olfactory bulbs. The circular fissure is prominent on endocasts of all the taxa we examined except *Tachyglossus* (Macrini et al., 2006), *Phascolarctos*, and *Vombatus* (Macrini et al., 2007); therefore, the MRCA of therians has a prominent fissure. However, because nonmammalian cynodonts have shallow circular fissures (Quiroga, 1980a,b; Macrini, 2006), the condition for this character is equivocal for the MRCA of mammals.

Character 5. Surface of cerebral hemisphere casts: lissencephalic (i.e., smooth; 0), or gyrencephalic (i.e., convoluted; 1). Among some groups of extant mammals, gyrencephaly of brains correlates with body weight, brain weight, and isocortex volume (e.g., von Bonin, 1941; Elias and Schwartz, 1971; Jerison, 1973, 1982; Zilles et al., 1989, and references within).

Lissencephalic endocasts usually result from skulls that contained small, lissencephalic cerebral hemispheres. However, some mammals with large, gyrencephalic brains such as hominids, proboscideans, and cetaceans, have smooth endocasts (e.g., Osborn, 1942; Edinger, 1955; Tobias, 1971; Jerison, 1973; Holloway et al., 2004; Colbert et al., 2005) because meninges, cisterns, and other soft-tissue structures of the endocranial cavity, fill in the spaces in the sulci of the brain, producing a smooth, flattened surface that contacts the skull bones.

When dealing with fossils, one can only assume that mammals with small endocranial cavities and lissencephalic endocasts actually had lissencephalic cerebral hemispheres. Data from brains of extant mammals can also be useful for drawing inferences about the surfaces of the cerebrum from fossil endocasts. Empirical data suggest that extant mammals with brain weights under 5 g, for the most part, have relatively smooth cerebral hemispheres (Bauchot and Stephan, 1967; Elias and Schwartz, 1971; Zilles et al., 1989; Striedter, 2005). Assuming that brain tissue has an average density of 1.0 g/cm^3 (following Jerison, 1973), *Vincelestes* had a brain weight of less than 2.4 g. The brain size data combined with the fact that the endocast is lissencephalic suggest that the cerebral hemispheres of *Vincelestes* were also lissencephalic.

The presence of lissencephalic endocasts is the plesiomorphic condition for Mammalia based on the endocasts of extinct mammals (Kielan-Jaworowska et al., 2004). Based on brains of extant mammals, gyrencephaly or the condition of having convoluted cerebral hemispheres has independently evolved several times in Placentalia, at least three times in Marsupialia, and at least once within Monotremata (Johnson, 1977; Nieuwenhuys et al., 1998; Striedter, 2005). This finding is corroborated using parsimony ancestral state reconstruction of the character on multiple topologies for major clades of extant mammals (e.g., Novacek, 1992; Horovitz and Sánchez-Villagra, 2003; Springer et al., 2005). Furthermore, the inferred ancestral pattern of fissurization varies between different extant mammalian groups (Nieuwenhuys et al., 1998). The presence of lissencephalic cerebral hemisphere casts was the likely condition for the MRCA of therians based on endocasts of the eutherians *Kennalestes*, *Barunlestes*, and *Zalambdalestes* (Kielan-Jaworowska, 1984, 1986); basal metatherians (e.g., *Pucadelphys*; Macrini et al., 2007); and *Vincelestes*.

Character 6. Rhinal fissure on endocast: absent (0), or present (1). The rhinal fissure is defined as the external border between the isocortex (i.e., neocortex) and the piriform cortex of the telencephalon of mammals (Jerison, 1973, 1991; Rowe, 1996a,b; Nieuwenhuys et al., 1998). The mammalian isocortex is the six-layered portion of the dorsal pallium (or neopallium) that receives sensory projections from other portions of the brain (Butler and Hodos, 1996; Nieuwenhuys et al., 1998).

The rhinal fissure is frequently used as a marker for the base of the isocortex in mammals (Jerison, 1973, 1991), but the fissure is not always visible on the endocasts of some mammals, making it difficult to track the expansion of the isocortex based on this feature alone. Lack of a rhinal fissure on a cranial endocast is not necessarily an indication of absence of isocortex, because the rhinal fissure is absent on the endocasts of extant taxa that clearly possess the fissure on the exteriors of their brains (Jerison, 1991; e.g., *Monodelphis domestica*, Macrini et al., 2007).

The ancestral condition for the MRCA of mammals and the MRCA of therians is to lack a rhinal fissure on endocasts. This finding may simply be an artifact of size, such that the rhinal fissure does not leave an impression on the endocasts of mammals with small brains.

Character 7. Lateral extent of cerebral hemisphere cast: most lateral point of cerebral cast is medial to or even with the parafloccular cast (0), or cerebral cast clearly extends laterally beyond parafloccular cast (1). *Vincelestes* exhibits the ancestral state (0) for this character and this finding is also the condition in the MRCA of therians.

Character 8. Superior sagittal sinus cast: not visible on dorsal surface of endocast (0), or visible (1). The sss does not appear on endocasts if it is located deep within the meninges (e.g., *Phascolarctos*) or if the walls of the sss are completely surrounded by bone such as an ossified falx cerebri, as is the case with *Vincelestes* and the extant dolphin *Tursiops truncatus* (Colbert et al., 2005). In the latter case, this character is correlated with character 9. The lack of an sss cast on the dorsal surface of an endocast (state 0) is reconstructed for the MRCA of therians.

Character 9. Ossified falx cerebri: absent (0), or present (1). The falx cerebri is a portion of the dura mater that occupies the median sulcus between the cerebral hemispheres. The ossified falx cerebri is examined

in this study because of the potential that it is correlated with the depth of the median sulcus on an endocast. This character is also potentially correlated with the visibility of the superior sagittal sinus cast on endocasts (character 8).

The falx cerebri is known to ossify in *Obdurodon dicksoni*, a Miocene platypus, and *Ornithorhynchus anatinus*, the extant platypus (Macrini et al., 2006), some extant cetaceans (e.g., dolphins and porpoises, Klintworth, 1968; Nojima, 1988; Colbert et al., 2005), sirenians (Nojima, 1988), some pinnipeds (Nojima, 1988), and *Vincelestes*. Calcification of the falx cerebri is also documented in humans, most commonly among the elderly (Cheon et al., 2002). To our knowledge, an ossified falx cerebri is not documented for any other extinct or extant mammalian taxon than those mentioned above.

Based on the current phylogenetic (e.g., Luo and Wible, 2005; Rose and Archibald, 2005) and anatomical information, the ossified falx cerebri is independently derived in each of these taxa. However, many stem therians have poorly preserved cranial material, and it is possible that, as better cranial material is found for these taxa, the distribution of this character may change.

The presence of an ossified falx cerebri is currently considered the derived condition based on the known distribution of this state within extant placentals. However, using the Luo and Wible (2005) tree, the current ancestral state reconstruction for the MRCA of mammals is equivocal for this character. Future examination of serial sections or CT images of skulls of nonmammalian cynodonts and additional nontherian mammals might support a reversal of the polarity of this character.

Character 10. Osseous tentorium: absent (0), represented by posteromedial ossification of tentorium cerebelli (1), lateral ossification of tentorium cerebelli (2), or complete ossification of tentorium cerebelli (3). Among extant mammals, an osseous tentorium is present in equids, carnivorans, pholidotes, cetaceans, and macropodid marsupials, but the degree of ossification of the tentorium cerebelli of the dura mater is variable among these taxa (Jollie, 1968; Klintworth, 1968; Bjerring, 1995; Solano and Brawer, 2004; Colbert et al., 2005). For example, in *Felis catus* (domestic cat), the entire tentorium cerebelli is ossified in adults (state 3), but in other mammals, only portions of the tentorium ossify (Klintworth, 1968). Only the posteromedial portion of the tentorium cerebelli ossifies (state 1) in some mammals such as the *Canis familiaris* (domestic dog), *Mustela vison* (mink), *Tursiops truncatus* (bottlenose dolphin), *Delphinus delphis* (common dolphin), *Phocoenoides dalli* (Dall's porpoise), *Equus caballus* (horse), and *Thylogale browni* (Brown's pademelon; Klintworth, 1968; Solano and Brawer, 2004). Only the lateral portions of the tentorium ossify (state 2) in *Manis* (pangolin; Jollie, 1968). In some extant mammals (e.g., carnivorans, macropodids, equids), the osseous tentorium is formed before adulthood, but in other mammals (e.g., delphinids and phocoenids), the ossification occurs during the course of adult aging (Nojima, 1988).

An osseous tentorium is also present, but damaged in the specimen of *Vincelestes* examined in this study (Fig. 5), the only documented occurrence of this osseous structure outside Theria. The osseous tentorium of *Vincelestes* represented a posteromedial ossification of the tentorium cerebelli (state 1).

The taxonomic distribution and differences in extent of ossification of the tentorium cerebelli suggest that the formation of an osseous tentorium was independently derived multiple times in Theriiformes. Lack of an osseous tentorium is the condition in the MRCA of therians and the MRCA of mammals.

Recognition of the variation of ossification of the osseous tentorium also has implications for higher level relationships within Placentalia. For example, molecular data routinely converge on a Carnivora and Pholidota sister relationship (Springer et al., 2005, and references within). Morphological support for this clade is weak, but one reported character supporting this relationship is the presence of an osseous tentorium in both carnivorans and pholidotes (e.g., Rose et al., 2005, and references within). As mentioned above, only the lateral portions of the tentorium cerebelli ossify in pangolins, whereas the medial portion or the entire tentorium ossifies in carnivorans. This morphological variation combined with the taxonomic distribution of an osseous tentorium suggests that presence of ossification of the tentorium cerebelli is plastic among mammals and is not a synapomorphy supporting the purported Carnivora and Pholidota sister relationship.

Character 11. Exposure of midbrain (superior and inferior colliculi) on dorsal surface of endocast: absent (0), or present (1). The midbrain is not exposed on several endocasts because of coverage by sinuses (e.g., transverse sinus) and associated meninges, a posteriorly expanded cerebrum, or a combination of these structures (Edinger, 1964; Nieuwenhuys et al., 1998). Lack of exposure of the colliculi on endocasts does not necessarily correlate with lack of exposure of these structures on the dorsal view of the brain. For example, *Didelphis virginiana* (Dom et al., 1970), *Monodelphis domestica* (Macrini et al., 2007), and *Tenrec ecaudatus* (Bauchot and Stephan, 1967), all have their colliculi exposed in dorsal view of their brains but not on the corresponding endocasts.

The colliculi are exposed on the dorsal surface of endocasts of at least a few mammalian endocasts, including the fossil eutherians *Asioryctes*, *Kennalestes*, *Zalambdalestes*, and *Barunlestes* (Kielan-Jaworowska, 1984, 1986; Kielan-Jaworowska and Trofimov, 1986), and at least a few extant placentals (Bauchot and Stephan, 1967). But the taxa possessing state (1) are definitely in the minority among the taxa we sampled. The condition for this character in *Vincelestes* is uncertain because of damage to the skull in this region. The MRCA of therians most likely did not have dorsal exposure of the midbrain on its endocast based on the distribution of this character among the sampled crown mammals. The polarization of this character is also supported by the current knowledge of the endocasts of nonmammalian cynodonts (Hopson, 1979; Quiroga, 1980a,b; Macrini, 2006).

Character 12. Cast of vermis of cerebellum: extends anterior to or even with the parafloccular casts (0), or vermis remains behind parafloccular casts (1). This char-

acter is modified from Luo and Wible (2005, character 415). State (0) is present in eutriconodontans (Simpson, 1927; Kielan-Jaworowska, 1986), the multituberculate *Kryptobaatar* (Kielan-Jaworowska and Lancaster, 2004), *Vincelestes*, *Pucadelphys* (Macrini et al., 2007), and *Phascolarctos*. In contrast, several crown therians including marsupials (Macrini et al., 2007), *Leptictis* (Novacek, 1982, 1986), and *Zalambdalestes* (Kielan-Jaworowska, 1984, 1986; Wible et al., 2004) have a small vermis cast that is positioned posterior to the parafloccular casts (state 1). The vermis was not observed on endocasts of nonmammalian cynodonts (Watson, 1913; Hopson, 1979; Quiroga, 1979, 1980a,b, 1984). Based on this distribution, the condition in the MRCA of therians is equivocal.

Character 13. Cerebellar hemisphere casts: not visible on endocast (0), or well-developed on endocast (1). This character is modified from Luo and Wible (2005, character 417). The cerebellar hemispheres are gross anatomical divisions of the mammalian cerebellum and do not necessarily reflect functional differences (Nieuwenhuys et al., 1998). Instead the hemispheres indicate lateral expansion of the cerebellum in mammals.

Cerebellar hemisphere casts are present on the endocast of *Vincelestes* as well as on endocasts of monotremes (Macrini et al., 2006) and crown therians (Kielan-Jaworowska, 1984, 1986; Novacek, 1986; Macrini et al., 2007). In contrast, cerebellar hemispheres are notably absent from endocasts of multituberculates (Kielan-Jaworowska, 1986) and nonmammalian cynodonts (Watson, 1913; Hopson, 1979; Quiroga, 1979, 1980a, b, 1984). Therefore, the presence of cerebellar hemispheres in the MRCA of therians is a plesiomorphic condition.

Character 14. Cast of the paraflocculus of the cerebellum: present on endocast (0), or absent from endocast (1). The degree to which the paraflocculus of the cerebellum filled the subarcuate fossa of *Vincelestes* is uncertain. A study of extant marsupials revealed that the paraflocculus fills at least a portion of the subarcuate space in all taxa examined, but to varying degrees in different taxa (Sánchez-Villagra, 2002). Based on extant phylogenetic bracketing (Witmer, 1995), at least a portion of this space was occupied by the paraflocculus in *Vincelestes*.

The presence of parafloccular lobes represented on endocasts is the plesiomorphic condition for the MRCA of therians. The paraflocculus is associated with coordination, balance, and vestibular sensory acquisition (Butler and Hodos, 1996; Nieuwenhuys et al., 1998).

Character 15. Percent of endocast composed by parafloccular casts: less than 1% (0), or greater than or equal to 1% (1). The parafloccular casts constitute approximately 1% of the total endocranial cavity on average for the taxa we examined. The MRCA of therians exhibits the ancestral character state (0). However, some crown therians such as *Dromiciops australis* (monito del monte [little mountain monkey]) and *Dasyurus hallucatus* (northern quoll) show the derived state.

Character 16. Parafloccular cast shape: cone-shaped (0), broad and rounded (1), large, posterolaterally oriented ovoid (2), or long and cylindrical without expansion on the distal end (3). Character states were determined from published descriptions of the subarcuate fossa of the petrosal, published descriptions of parafloccular casts of endocasts, and examination of digital endocasts (Kermack, 1963; MacIntyre, 1972; Novacek, 1982, 1986, 1989; Kielan-Jaworowska, 1984, 1986; Wible, 1990; Rougier et al., 1992, 1996; Wible and Rougier, 2000; Luo et al., 2002; Sánchez-Villagra, 2002; Kielan-Jaworowska and Lancaster, 2004).

Presence of cone-shaped parafloccular casts is the inferred ancestral state because it occurs in some nonmammalian mammaliaformes (Macrini, 2006). The MRCA of therians and the MRCA of mammals is reconstructed with broad and rounded parafloccular casts (state 1).

Character 17. Depth of hypophyseal fossa relative to its length: fossa deeper than long (aspect ratio > 1.1) (0), fossa longer than deep (aspect ratio < 0.9) (1), or hypophyseal fossa depth and length approximately equal (aspect ratio $= 0.9$–1.1) (2). The hypophyseal fossa is a poor indicator of the size and shape of the pituitary gland in many mammals (Edinger, 1942), but we are confident that at least a portion of this space was occupied by the gland in *Vincelestes*. Based on distribution of this character in nonmammalian cynodonts, presence of a fossil that is deeper than wide is the plesiomorph condition (MaCrini, 2006). The condition for this character in the MRCA of therians is equivocal.

Character 18. Width of hypophyseal fossa relative to its length: wider than long (aspect ratio > 1.1) (0), longer than wide (aspect ratio < 0.9) (1), or hypophyseal fossa width and length approximately equal (aspect ratio $= 0.9$–1.1) (2). The presence of a hypophyseal fossa that is wider than long is the ancestral state for this character, based on the condition in nonmammalian cynodonts (Macrini, 2006). Therefore, presence of this condition (state 0) in the MRCA of therians is plesiomorphic.

Character 19. Position of aperture of canals transmitting the carotid arteries into the hypophysis: located in posterolateral portion of hypophysis (0), or anterolateral portion of hypophysis (1). The MRCA of therians exhibits state (0) for this character.

Character 20. Cavum epiptericum: confluent with cavum supracochleare (0), or cavum epiptericum and cavum supracochleare separated by at least a partial bony wall (1). This character was taken from Wible (1990).

The cavum epiptericum is the space between the primary and secondary braincase walls of mammals. In nonmammalian cynodonts, the medial wall of the cavum epiptericum is formed by the pila antotica, an anterior extension of the prootic, which acts as the primary wall of the endocranial cavity (Presley, 1980; Maier, 1987; Novacek, 1993; Rougier and Wible, 2006). The primary bony wall of crown mammals is greatly reduced and the cavum epiptericum is incorporated in the endocranial cavity (Kühn and Zeller, 1987; Novacek, 1993). There-

fore, the lateral wall of the cavum epiptericum forms the secondary wall of the braincase in crown mammals and the composition of this wall is an important source of phylogenetic data among crown mammals (see discussions in Presley, 1980; Kühn and Zeller, 1987; Maier, 1987; Hopson and Rougier, 1993; Novacek, 1993; Kielan-Jaworowska et al., 2004).

The contents of the cavum epiptericum are variable among extant mammals. The cavum epiptericum of *Ornithorhynchus anatinus*, the platypus, houses the semilunar (Gasserian) ganglion of the trigeminal nerve (V), a portion of the otic ganglion, the geniculate ganglion (for cranial nerve VII), and portions of cranial nerves III–VII (Zeller, 1989b). However, in *Tachyglossus aculeatus*, the short-nosed echidna, the sphenopalatine ganglion for the greater petrosal nerve is also incorporated in the cavum epiptericum but the geniculate ganglion remains extracranial (Kühn and Zeller, 1987). In extant therians, the sphenopalatine and otic ganglia are extracranial but the geniculate ganglion is typically housed in the separate cavum supracochleare of the petrosal bone (Kühn and Zeller, 1987; Rougier et al., 1996).

The posterior wall of the cavum epiptericum of *Vincelestes* is pierced by an opening (fenestra semilunaris), which connects with the cavum supracochleare (Rougier et al., 1992). According to Rougier et al. (1992), the fenestra semilunaris was probably covered by a dense fibrous connective tissue that did not permit transmission of major structures between the two cava. Therefore, based on the cranial osteology and on extant phylogenetic bracketing, the cavum epiptericum of *Vincelestes* likely housed the semilunar ganglion and portions of several cranial nerves, but not the geniculate ganglion.

The presence of at least a partial bony separation of the cavum epiptericum and cavum supracochleare is a synapomorphy for the least inclusive clade containing *Vincelestes* and Theria. However, this is not an unequivocal synapomorphy because the cavum supracochleare is also separate from the cavum epiptericum in *Tachyglossus* (Kühn and Zeller, 1987) and Eutriconodonta (Kermack, 1963). The presence of a fenestra semilunaris in *Vincelestes*, at least one other stem therian (Wible et al., 1995), some extant marsupials (Wible, 1990), and "zhelestid" eutherians (Ekdale et al., 2004) suggests this feature should also be reconstructed for the MRCA of therians.

Character 21. Anterior portion of cavum epiptericum leading to the sphenorbital fissure: anterior portions of right and left cava are at least partially separated at sphenorbital fissure (0), or cava are completely confluent at sphenorbital fissure (1). The MRCA of therians is reconstructed as having the anterior portions of the right and left cava at least partially separated contrary to the derived condition seen in *Vincelestes*. In at least some crown therians (e.g., *Monodelphis domestica*), the presphenoid forms a partial barrier between the portion of the right and left cava leading to the sphenorbital fissures.

Encephalization Quotients

An encephalization quotient (EQ) is the ratio of actual to expected brain sizes for a particular taxon (Jerison, 1973). Expected brain size is calculated using equations relating brain mass (or endocranial volume) to body mass; these equations are determined by comparison of these variables among several closely related taxa (Jerison, 1973). Encephalization quotients are widely used in the literature but also frequently criticized (e.g., Deacon, 1990; Striedter, 2005). Even so, EQs are useful for determining allometric relationships between endocranial volume and body mass for extinct animals. In addition, the degree of encephalization in mammals appears to correlate with several anatomical and functional variables (Jerison, 1973; Eisenberg and Wilson, 1978, 1981).

TABLE 4. Encephalization quotient values for *Vincelestes*[a]

	EV/(0.12 [Wt]$^{0.67}$)[b]	EV/(0.055 [Wt]$^{0.74}$)[c]
EQ (with olfactory bulbs)[d]	0.27	0.37
EQ (without olfactory bulbs)[e]	0.24	0.33

[a]EQ, encephalization quotient; EV, endocranial volume; Wt, weight or body mass (body mass estimated as 619 g for MACN-N 04).
[b]Equation from Jerison (1973).
[c]Equation from Eisenberg (1981).
[d]Endocranial volume with olfactory bulbs = 2.371 ml.
[e]Endocranial volume without olfactory bulbs = 2.115 ml.

In this study, we do not address methodological issues associated with encephalization quotients, but instead compare the EQ calculated for *Vincelestes* (Table 4) with those EQs determined from several fossil and extant crown mammals. We make comparisons between EQs calculated using the equation of Eisenberg (1981), because this equation was determined using a large amount of empirical data from a wide range of extant mammalian taxa. We also include the olfactory bulb casts in the determination of endocranial volume when comparing EQs of different taxa. Exclusion of the olfactory bulb casts when determining the endocranial volume is unjustified, because the olfactory bulbs receive olfactory sensory input and process that information to a certain degree and as such are part of the brain (Nieuwenhuys et al., 1998; Rowe et al., 2005). Furthermore, it is not possible to accurately determine the volume of the olfactory bulb casts for many endocranial volumes provided in the literature. However, for the sake of completeness, we calculated EQ for *Vincelestes* using both endocranial volumes that include and exclude the olfactory bulb casts volume, and using two different EQ equations (Table 4).

The EQ for *Vincelestes* calculated using the total endocranial volume, a body mass of 619 g, and the Eisenberg (1981) equation for the one specimen examined in this study is 0.37. The EQ for *Vincelestes* overlaps the lower range of EQs calculated for basal eutherians (0.36–0.80; Novacek, 1982, 1986; Kielan-Jaworowska, 1984, 1986), and surpasses EQs calculated for the metatherian *Pucadelphys* (0.32) and *Didelphis virginiana* (0.34; Macrini et al., 2007). Therefore, the relative brain size of *Vincelestes* is close to the bottom range of EQs for crown therians.

However, the EQs of multituberculates (0.54–0.64; Kielan-Jaworowska, 1983; Krause and Kielan-Jaworowska, 1993) and eutriconodontans (0.49; Jerison, 1973)

are higher than the EQ of *Vincelestes*. In addition, crown monotremes have considerably higher EQs (0.75–1.00; Macrini et al., 2006) than *Vincelestes*, as do at least some crown marsupials (Eisenberg and Wilson, 1981; Macrini et al., 2007). This finding suggests that relatively large brains evolved multiple times within Mammalia, particularly within Theriimorpha, the clade containing multituberculates, eutriconodontans, *Vincelestes*, and crown therians (Fig. 1).

However, the taxonomic sampling for these data is sparse, and EQs for different taxa might be modified in the future as methodologies for determining endocranial volumes and body masses are standardized. For example, some of the discrepancy between the EQs determined for *Vincelestes* and other extinct mammals (e.g., multituberculates, eutriconodontans, basal eutherians) might result from methodological differences in determining endocranial volume (e.g., estimating from natural endocasts versus measuring on digital endocasts) and estimating body mass. In addition, the effects of phylogenetic nonindependence have not been examined for these data (Felsenstein, 1985; Harvey and Pagel, 1991). These and other problems associated with EQs need to be addressed in future studies to properly examine the evolution of brain size across the major lineages of mammals.

CONCLUSIONS

In this study, we provided new anatomical data on the endocranial cavity of *Vincelestes* through the study of a digital endocast, the first endocast described for this taxon. The endocast of *Vincelestes* adds to a growing library of digital cranial endocasts from extinct and extant mammals (e.g., Marino et al., 2000, 2003; Colbert et al., 2005; Macrini et al., 2006, 2007) and adds to existing information on natural and artificial endocasts of mammals (e.g., Simpson, 1927; Edinger, 1948, 1955; Tobias, 1971; Jerison, 1973; Radinsky, 1968, 1973, 1975, 1977, 1978, 1981; Novacek, 1982, 1986; Kielan-Jaworowska, 1983, 1984, 1986; Krause and Kielan-Jaworowska, 1993; Holloway et al., 2004; Kielan-Jaworowska and Lancaster, 2004; Kielan-Jaworowska et al., 2004), and nonmammalian cynodonts (e.g., Watson, 1913; Hopson, 1979; Quiroga, 1979, 1980a,b, 1984). Examination of digital, natural, and artificial endocasts in combination allows for the study of brain evolution across the clade Mammalia. Comparison of the endocast of *Vincelestes* with endocasts of extinct and extant mammals allows ancestral character state reconstructions for the MRCA of therians, facilitating study of the evolution of the brain among basal crown therians.

Based on the taxa we examined, none of the endocranial characters was a synapomorphy that diagnosed the clade Theria. Instead, the brain of the MRCA of therians is reconstructed as possessing several plesiomorphic states, at least for these characters, which are visible on cranial endocasts. Specifically, we found the following character states to be plesiomorphic for Theria. The olfactory bulb casts are large and separated from the rest of the endocast by a prominent circular fissure. The surfaces of the cerebral hemisphere casts and presumably the actual cerebrum were lissencephalic. A rhinal fissure is not visible on endocasts. The cerebral hemisphere casts do not extend lateral to the cast of the paraflocculus. The superior sagittal sinus and the midbrain are not represented on the endocast dorsal surface. An osseous tentorium is absent. The cerebellar hemisphere casts are present as are small parafloccular casts with broad, rounded termini. The hypophyseal fossa is wider than it is long, and the opening of the canals transmitting the carotid arteries occurs in the posterolateral portion of the fossa. The cavum epiptericum and cavum supracochleare are separated by a bony wall, which was probably pierced by a fenestra semilunaris. The anterior portions of the right and left cava epipterica at the level of the sphenorbital fissure are at least partially separated by a bony partition.

The lack of neuroanatomical synapomorphies diagnosing Theria that are distinguishable from endocasts might seem to suggest that the brain in basal therians is conserved relative to more basal mammals. However, comparative study of the brains of extant mammals revealed synapomorphies for Theria based on neuroanatomy not visible on endocasts (Johnson et al., 1982a,b, 1994). For example, therians have a complete secondary somatic sensory (SII) projection region of the cerebral cortex, but monotremes have only the primary somatic sensory (SI) projection region (Johnson et al., 1994). The fibers of the optic tract run under a superficial gray layer in most therians as opposed to the plesiomorphic condition in which the optic tract fibers run superficially over the anterior tectum (Johnson et al., 1982a,b). Finally, the external cuneate nucleus is clearly separated from the cuneate–gracile complex of the medulla oblongata (Johnson et al., 1994).

There is a long recognized need to incorporate more data from the brain, as inferred from cranial endocasts, into phylogenetic analyses of the relationships of extinct and extant mammals (Kermack and Kermack, 1984; Kielan-Jaworowska, 1997). Some phylogenetic analyses have included a few endocranial characters (e.g., Luo et al., 2002, 2003; Kielan-Jaworowska et al., 2004; Luo and Wible, 2005), but we encourage authors to also incorporate the characters presented here in future analyses. Although none of these endocranial characters diagnoses Theria, the characters might be useful for diagnosing larger clades (e.g., Mammalia) when the relevant outgroups are examined. Conversely, the endocranial characters presented in this study can introduce a source of conflict between purported higher level relationships within Mammalia, as is the case with the ossification of the tentorium cerebelli (character 10).

ACKNOWLEDGMENTS

The skull of *Vincelestes* was scanned by Cambria Denison at the UTCT. A segment of this study formed a portion of T. Macrini's dissertation submitted in partial fulfillment of the requirements for the degree of Doctor of Philosophy at The University of Texas at Austin. We thank Chris J. Bell, Dave Cannatella, Rich Cifelli, Zhe-Xi Luo, Jim Sprinkle, and two anonymous readers for critical review of earlier versions of this study. All authors were funded by the National Science Foundation, and G.W.R. was funded by the Antorchas Foundation.

LITERATURE CITED

Alexander RM, Jayes AS, Maloiy GMO, Wathuta EM. 1979. Allometry of the limb bones of mammals from shrews (*Sorex*) to elephant (*Loxodonta*). J Zool (Lond) 189:305–314.

Ax P. 1985. Stem species and the stem lineage concept. Cladistics 1:279–287.

Bauchot R, Stephan H. 1967. Encéphales et moulages endocraniens de quelques insectivores et primates actuels. In: Problemes actuels de paleontologie (Evolution des Vertebres): Colloques Internationaux du Centre National de la Recherche Scientifique. Paris, France, 6–11 June 1966. Editions du Centre National de la Recherche Scientifique 163:575–586.

Bjerring HC. 1995. The parietal problem: how to cut this Gordian knot? Acta Zool (Stockh) 76:193–203.

Bonaparte JF. 1986. Sobre *Mesungulatum houssayi* y nuevos mamíferos Cretácicos de Patagonia. Actas IV Congreso Argentino Paleontologia, y Bioestratigrafía 2:48–61.

Bonaparte JF, Rougier GW. 1987. Mamiferos del Cretacico inferior de Patagonia. IV Congreso Latinoamericano de Paleontología, Bolivia 1:343–359.

Butler H. 1967. The development of mammalian dural venous sinuses with especial reference to the post-glenoid vein. J Anat 102:33–56.

Butler AB, Hodos W. 1996. Comparative vertebrate neuroanatomy: evolution and adaptation. New York: Wiley-Liss. 514 p.

Cheon J-E, Kim J-E, Yang HJ. 2002. CT and pathologic findings of a case of subdural osteoma. Korean J Radiol 3:211–213.

Colbert MW, Racicot R, Rowe T. 2005. Anatomy of the cranial endocast of the bottlenose dolphin *Tursiops truncatus*, based on HRXCT. J Mammal Evol 12:195–207.

Deacon TW. 1990. Rethinking mammalian brain evolution. Am Zool 30:629–705.

Denison C, Carlson WD, Ketcham RA. 1997. Three-dimensional quantitative textural analysis of metamorphic rocks using high-resolution computed X-ray tomography: Part I. Methods and techniques. J Metamorph Geol 15:29–44.

de Queiroz K, Gauthier J. 1990. Phylogeny as a central principle in taxonomy: phylogenetic definitions of taxon names. Syst Zool 39:307–322.

Dom R, Fisher BL, Martin GF. 1970. The venous system of the head and neck of the opossum (*Didelphis virginiana*). J Morphol 132:487–496.

Edinger T. 1942. The pituitary body in giant animals fossil and living: a survey and a suggestion. Q Rev Biol 17:31–45.

Edinger T. 1948. Evolution of the horse brain. Geol Soc Am Memoir 25:1–177.

Edinger T. 1955. Hearing and smell in cetacean history. Mschr Psychiat Neurol 129:37–58.

Edinger T. 1964. Midbrain exposure and overlap in mammals. Am Zool 4:5–19.

Eisenberg JF. 1981. The mammalian radiations. Chicago: University of Chicago Press. 610 p.

Eisenberg JF, Wilson DE. 1978. Relative brain size and feeding strategies in the Chiroptera. Evolution 32:740–751.

Eisenberg JF, Wilson DE. 1981. Relative brain size and demographic strategies in didelphid marsupials. Am Nat 118:1–15.

Ekdale EG, Archibald JD, Averianov AO. 2004. Petrosal bones of placental mammals from the Late Cretaceous of Uzbekistan. Acta Palaeontol Pol 49:161–176.

Elias H, Schwartz D. 1971. Cerebro-cortical surface areas, volumes, lengths of gyri and their independence in mammals, including man. Z Saugetierkunde 36:147–163.

Evans HE. 1993. Miller's anatomy of the dog. 3rd ed. Philadelphia: WB Saunders Co.1130 p.

Felsenstein J. 1985. Phylogenies and the comparative method. Am Nat 125:1–15.

Flynn JJ, Wyss AR. 1999. New marsupials from the Eocene-Oligocene transition of the Andean main range, Chile. J Vertebr Paleontol 19:533–549.

Harvey PH, Pagel MD. 1991. The comparative method in evolutionary biology. New York: Oxford University Press. 239 p.

Holloway RL, Broadfield DC, Yuan MS. 2004. The human fossil record. Volume 3. Brain endocasts; the paleoneurological evidence. New York: Wiley-Liss. 315 p.

Hopson JA. 1979. Paleoneurology. In: Gans C, Northcutt RG, Ulinski P, editors. Biology of the Reptilia. Vol. 9. Neurology A. London: Academic Press. p 39–146.

Hopson JA, Rougier GW. 1993. Braincase structures in the oldest known skull of a therian mammal: implications for mammalian systematics and cranial evolution. Am J Sci 293A:268–299.

Horovitz I. 2000. The tarsus of *Ukhaatherium nessovi* (Eutheria, Mammalia) from the Late Cretaceous of Mongolia: an appraisal of the evolution of the ankle in basal therians. J Vertebr Paleontol 20:547–560.

Horovitz I. 2003. Postcranial skeleton of *Ukhaatherium nessovi* (Eutheria, Mammalia) from the Late Cretaceous of Mongolia. J Vertebr Paleontol 23:857–868.

Horovitz I, Sánchez-Villagra MR. 2003. A morphological analysis of marsupial mammal higher-level phylogenetic relationships. Cladistics 19:181–212.

Jerison HJ. 1973. Evolution of the brain and intelligence. New York: Academic Press. 482 p.

Jerison HJ. 1982. Allometry, brain size, cortical surface, and convolutedness. In: Armstrong E, Falk D, editors. Primate brain evolution: methods and concepts. New York: Plenum Press. p 77–84.

Jerison HJ. 1991. Fossil brains and the evolution of the neocortex. In: Finlay BL, Innocenti G, Scheich H, editors. The neocortex: ontogeny and phylogeny. NATO Advanced science institutes series A: life sciences Vol. 200:5–19. New York: Plenum Press.

Johnson JI. 1977. Central nervous system of marsupials. In: Hunsaker D, editor. The biology of marsupials. New York: Academic Press. p 157–278.

Johnson JI, Switzer RC, Kirsch JAW. 1982a. Phylogeny through brain traits: fifteen characters which adumbrate mammalian genealogy. Brain Behav Evol 20:72–83.

Johnson JI, Switzer RC, Kirsch JAW. 1982b. Phylogeny through brain traits: the distribution of categorizing characters in contemporary mammals. Brain Behav Evol 20:97–117.

Johnson JI, Kirsch JAW, Reep RL, Switzer RC. 1994. Phylogeny through brain traits: more characters for the analysis of mammalian evolution. Brain Behav Evol 43:319–347.

Jollie M. 1968. The head skeleton of a new-born *Manis javanica* with comments on the ontogeny and phylogeny of the mammal head skeleton. Acta Zool 49:227–305.

Kermack KA. 1963. The cranial structure of the triconodonts. Philos Trans R Soc B 246:83–103.

Kermack DM, Kermack KA. 1984. The evolution of mammalian characters. Washington, DC: Kapitan Szabo Publishers. 149 p.

Kielan-Jaworowska Z. 1983. Multituberculate endocranial casts. Palaeovertebrata 13:1–12.

Kielan-Jaworowska Z. 1984. Evolution of the therian mammals in the Late Cretaceous of Asia. VI. Endocranial casts of eutherian mammals. Palaeontol Pol 46:157–171.

Kielan-Jaworowska Z. 1986. Brain evolution in Mesozoic mammals. In: Flanagan KM, Lillegraven JA, editors. Vertebrates, phylogeny, and philosophy. Contributions to geology, special paper 3. Laramie: University of Wyoming. p 21–34.

Kielan-Jaworowska Z. 1997. Characters of multituberculates neglected in phylogenetic analyses of early mammals. Lethaia 29:249–266.

Kielan-Jaworowska Z, Lancaster TE. 2004. A new reconstruction of multituberculate endocranial casts and encephalization quotient of *Kryptobaatar*. Acta Palaeontol Pol 49:177–188.

Kielan-Jaworowska Z, Trofimov BA. 1986. Endocranial cast of the Cretaceous eutherian mammal *Barunlestes*. Acta Palaeontol Pol 31:137–144.

Kielan-Jaworowska Z, Presley R, Poplin C. 1986. The cranial vascular system in taeniolabidoid multituberculate mammals. Philos Trans R Soc B 313:525–602.

Kielan-Jaworowska Z, Cifelli RL, Luo Z-X. 2004. Mammals from the age of dinosaurs: origins, evolution, and structure. New York: Columbia University Press. 630 p.

Klintworth GK. 1968. The comparative anatomy and phylogeny of the tentorium cerebelli. Anat Rec 160:635–642.
Krause DW, Kielan-Jaworowska Z. 1993. The endocranial cast and encephalization quotient of *Ptilodus* (Multituberculata, Mammalia). Palaeovertebrata 22:99–112.
Kühn HJ, Zeller U. 1987. The cavum epiptericum in monotremes and therian mammals. In: Kuhn HJ, Zeller U, editors. Morphogenesis of the mammalian skull. Berlin: Verlag Paul Parey. p 51–70.
Legarreta L, Uliana MA. 1999. El Jurásico y Cretácico de la Cordillera Principal y la Cuenca Neuquina. 1. Facies sedimentarias. In: Caminos R, editor. Geologia Argentina. Buenos Aires, Argentina: Segemar.Anales 29:399–416.
Loo YT. 1930. The forebrain of the opossum, *Didelphis virginiana*. J Comp Neurol 51:13–64.
Luo Z-X, Wible JR. 2005. A late Jurassic digging mammal and early mammalian diversity. Science 308:103–107.
Luo Z-X, Crompton AW, Sun A-L. 2001. A new mammaliaform from the Early Jurassic and evolution of mammalian characteristics. Science 292:1535–1540.
Luo Z-X, Kielan-Jaworowska Z, Cifelli RL. 2002. In quest for a phylogeny of Mesozoic mammals. Acta Palaeontol Pol 47:1–78.
Luo Z-X, Ji Q, Wible JR, Yuan C-X. 2003. An early Cretaceous tribosphenic mammal and metatherian evolution. Science 302:1934–1940.
Lyras GA, van der Geer AAE. 2003. External brain anatomy in relation to the phylogeny of Caninae (Carnivora: Canidae). Zool J Linn Soc 138:505–522.
MacIntyre GT. 1972. The trisulcate petrosal pattern of mammals. In: Dobzhansky T, Hecht MK, Steere WC, editors. Evolutionary biology. Vol. 6. New York: Appleton-Century-Crofts. p 275–303.
MacLeod N, Forey PL, editors. 2002. Morphology, shape and phylogeny. New York: Taylor and Francis. 308 p.
Macrini TE. 2006. The evolution of endocranial space in mammals and non-mammalian cynodonts. PhD dissertation, University of Texas, Austin. 278 p.
Macrini TE, Rowe T, Archer M. 2006. Description of a cranial endocast from a fossil platypus, *Obdurodon dicksoni* (Monotremata, Ornithorhynchidae), and the relevance of endocranial characters to monotreme monophyly. J Morphol 267:1000–1015.
Macrini TE, Muizon C, Cifelli RL, Rowe T. 2007. Digital cranial endocast of *Pucadelphys andinus*, a Paleocene metatherian. J Vertebr Paleontol 27:99–107.
Maddison WP, Maddison DR. 2006. Mesquite: a modular system for evolutionary analysis. Version 1.12. http://mesquiteproject.org.
Maier W. 1987. The ontogenetic development of the orbitotemporal region of the skull of *Monodelphis domestica* (Didelphidae, Marsupialia), and the problem of the mammalian alisphenoid. Mammalia Depicta 13:71–90.
Marino L. 2004. Cetacean brain evolution: multiplication generates complexity. Int J Comp Psychol 17:1–16.
Marino L, Uhen MD, Frohlich B, Aldag JM, Blane C, Bohaska D, Whitmore FC. 2000. Endocranial volume of Mid-Late Eocene archaeocetes (Order: Cetacea) revealed by computed tomography: implications for cetacean brain evolution. J Mammal Evol 7:81–94.
Marino L, Uhen MD, Pyenson ND, Frohlich B. 2003. Reconstructing cetacean brain evolution using computed tomography. Anat Rec 272B:107–117.
Marsh OC. 1884. Dinocerata. A monograph of an extinct order of gigantic mammals. Monogr US Geol Surv 10:1–237.
Marshall LG, Muizon C de. 1995. Part II. The skull. In: de Muizon C, editor. *Pucadelphys andinus* (Marsupialia, Mammalia) from the early Paleocene of Bolivia. Mem Mus Natl Hist Nat 165:21–90.
Meisami E, Bhatnagar KP. 1998. Structure and diversity in mammalian accessory olfactory bulb. Microsc Res Tech 43:476–499.
Meng J, Fox RC. 1995. Therian petrosals from the Oldman and Milk River Formations (Late Cretaceous), Alberta, Canada. J Vertebr Paleontol 15:122–130.
Negus V. 1958. The comparative anatomy and physiology of the nose and paranasal sinuses. London: E&S Livingstone Ltd. 402 p.
Nieuwenhuys R, Ten Donkelaar HJ, Nicholson C. 1998. The central nervous system of vertebrates. Berlin: Springer Verlag. 3 volumes, 2219 p.
Nojima T. 1988. Developmental patterns of the bony falx and bony tentorium of spotted dolphins (*Stenella attenuata*) and the relationship between degree of development and age. Mar Mammal Sci 4:312–322.
Novacek MJ. 1982. The brain of *Leptictis dakotensis*, an Oligocene leptictid (Eutheria: Mammalia) from North America. J Paleontol 56:1177–1186.
Novacek MJ. 1986. The skull of leptictid insectivorans and the higher-level classification of eutherian mammals. Bull Am Mus Nat Hist 183:1–112.
Novacek MJ. 1989. Higher mammal phylogeny: the morphological-molecular synthesis. In: Fernholm B, Bremer K, Jornvall H, editors. The hierarchy of life: molecules and morphology in phylogenetic analysis. New York: Elsevier Science Publishers. p 421–435.
Novacek MJ. 1992. Mammal phylogeny: shaking the tree. Nature 356:121–125.
Novacek MJ. 1993. Patterns of diversity in the mammalian skull. In: Hanken J, Hull BK, editors. The skull. Vol. 2. Patterns of structural and systematic diversity. Chicago: University of Chicago Press. p 438–545.
Novacek MJ, Rougier GW, Wible JR, McKenna MC, Dashzeveg D, Horovitz I. 1997. Epipubic bones in eutherian mammals from the Late Cretaceous of Mongolia. Nature 389:483–486.
Osborn HF. 1942. Proboscidea. Volume II. Stegodontoidea and Elephantoidea. New York: American Museum of Natural History Press. p 805–1675.
Pirlot P, Nelson J. 1978. Volumetric analysis of monotreme brains. Aust Zool 20:171–179.
Presley R. 1980. The braincase in Recent and Mesozoic therapsids. Mem Soc Geol Fr 139:159–162.
Quiroga JC. 1979. The brain of two mammal-like reptiles (Cynodontia- Therapsida). J Hirnforsch 20:341–350.
Quiroga JC. 1980a. Sobre un molde endocraneano del cinodonte *Probainognathus jenseni* Romer, 1970 (Reptilia, Therapsida), de la Formacion Ischichuca (Triasico medio), La Rioja, Argentina. Ameghiniana 17:181–190.
Quiroga JC. 1980b. The brain of the mammal-like reptile *Probainognathus jenseni* (Therapsida, Cynodontia). A correlative paleoneurological approach to the neocortex at the reptile-mammal transition. J Hirnforsch 21:299–336.
Quiroga JC. 1984. The endocranial cast of the advanced mammal-like reptile *Therioherpeton cargnini* (Therapsida- Cynodontia) from the Middle Triassic of Brazil. J Hirnforsch 25:285–290.
Radinsky L. 1968. Evolution of somatic sensory specialization in otter brains. J Comp Neurol 134:495–506.
Radinsky L. 1973. Are stink badgers skunks? Implications of neuroanatomy for mustelid phylogeny. J Mammal 54:585–593.
Radinsky L. 1975. Viverrid neuroanatomy: phylogenetic and behavioral implications. J Mammal 56:130–150.
Radinsky L. 1977. Brains of early carnivores. Paleobiology 3:333–349.
Radinsky L. 1978. Evolution of brain size in carnivores and ungulates. Am Nat 112:815–831.
Radinsky L. 1981. Brain evolution in extinct South American ungulates. Brain Behav Evol 18:169–187.
Rose KD, Archibald JD, editors. 2005. The rise of placental mammals: origins and relationships of the major extant clades. Baltimore, MD: Johns Hopkins University Press. 259 p.
Rose KD, Emry RJ, Gaudin TJ, Storch G. 2005. Xenarthra and Pholidota. In: Rose KD, Archibald JD, editors. The rise of placental mammals: origins and relationships of the major extant clades. Baltimore, MD: Johns Hopkins University Press. p 106–126.
Rougier GW. 1993. *Vincelestes neuquenianus* Bonaparte (Mammalia, Theria), un primitivo mamífero del Cretácico Inferior de la Cuenca Neuquina. PhD dissertation, University of Buenos Aires. 3 volumes, 720 p.
Rougier GW, Wible JR. 2006. Major changes in the ear region and basicranium of early mammals. In: Carrano MT, Gaudin TJ, Blob RW, Wible JR, editors. Amniote paleobiology: perspectives on the

evolution of mammals, birds, and reptiles. Chicago: University of Chicago Press. p 269–311.
Rougier GW, Wible JR, Hopson JA. 1992. Reconstruction of the cranial vessels in the early Cretaceous mammal *Vincelestes neuquenianus*: implications for the evolution of the mammalian cranial vascular system. J Vertebr Paleontol 12:188–216.
Rougier GW, Wible JR, Hopson JA. 1996. Basicranial anatomy of *Priacodon fruitaensis* (Triconodontidae, Mammalia) from the late Jurassic of Colorado, and a reappraisal of mammaliaform interrelationships. Am Mus Novit 3183:1–38.
Rougier GW, Wible JR, Novacek MJ. 1998. Implications of *Deltatheridium* specimens for early marsupial history. Nature 396:459–463.
Rougier GW, Wible JR, Novacek MJ. 2004. New specimens of *Deltatheroides cretacicus* (Metatheria, Deltatheroida) from the Late Cretaceous of Mongolia. In: Dawson MR, Lillegraven JA, editors. Fanfare for an uncommon paleontologist: papers in honor of Malcolm C. McKenna. Bull Carneg Mus Nat Hist 36:245–266.
Rowe T. 1988. Definition, diagnosis, and origin of Mammalia. J Vertebr Paleontol 8:241–264.
Rowe T. 1993. Phylogenetic systematics and the early history of mammals. In: Szalay FS, Novacek MJ, McKenna MC, editors. Mammalian phylogeny. Vol. 1. Mesozoic differentiation, multituberculates, monotremes, early therians, and marsupials. New York: Springer-Verlag. p 129–145.
Rowe T. 1996a. Brain heterochrony and origin of the mammalian middle ear. In: Ghiselin M, Pinna G, editors. New perspectives on the history of Life. San Francisco: California Academy of Sciences, Memoir 20. p 71–95.
Rowe T. 1996b. Coevolution of the mammalian middle ear and neocortex. Science 273:651–654.
Rowe T, Carlson W, Bottorff W. 1995. *Thrinaxodon*: digital atlas of the skull. (CD-ROM) 2nd ed. Austin: University of Texas Press.
Rowe TB, Eiting TP, Macrini TE, Ketcham RA. 2005. Organization of the olfactory and respiratory skeleton in the nose of the gray short-tailed opossum *Monodelphis domestica*. J Mammal Evol 12:303–336.
Sánchez-Villagra MR. 2002. The cerebellar paraflocculus and the subarcuate fossa in *Monodelphis domestica* and other marsupial mammals–ontogeny and phylogeny of a brain-skull interaction. Acta Theriol 47:1–14.
Simpson GG. 1927. Mesozoic Mammalia. IX. The brain of Jurassic mammals. Am J Sci 214:259–268.
Solano M, Brawer RS. 2004. CT of the equine head: technical considerations, anatomical guide, and selected diseases. Clin Tech Equine Pract 4:374–388.
Springer MS, Murphy WJ, Eizirik E, O'Brien SJ. 2005. Molecular evidence for major placental clades. In: Rose KD, Archibald JD, editors. The rise of placental mammals: origins and relationships of the major extant clades. Baltimore, MD: Johns Hopkins University Press. p 37–49.
Striedter GF. 2005. Principles of brain evolution. Sunderland, MA: Sinauer Associates. 436 p.
Tobias PV. 1971. The brain in hominid evolution. New York: Columbia University Press. 170 p.
von Bonin G. 1941. Side lights on cerebral evolution: brain size of lower vertebrates and degree of cortical folding. J Gen Psychol 25:273–282.
Wang Y, Hu Y, Meng J, Li C. 2001. An ossified Meckel's cartilage in two Cretaceous mammals and origin of the mammalian middle ear. Science 294:357–361.
Watson DMS. 1913. Further notes on the skull, brain, and organs of special sense of *Diademodon*. Ann Mag Nat Hist, Series 8 12:217–228.
Wible JR. 1990. Petrosals of Late Cretaceous marsupials from North America, and a cladistic analysis of the petrosal in therian mammals. J Vertebr Paleontol 10:183–205.
Wible JR, Hopson JA. 1993. Basicranial evidence for early mammal phylogeny. In: Szalay FS, Novacek MJ, McKenna MC, editors. Mammalian phylogeny. Vol. 1. Mesozoic differentiation, multituberculates, monotremes, early therians, and marsupials. New York: Springer-Verlag. p 45–62.
Wible JR, Rougier GW. 2000. Cranial anatomy of *Kryptobaatar dashzevegi* (Mammalia, Multituberculata), and its bearing on the evolution of mammalian characters. Bull Am Mus Nat Hist 247: 1–124.
Wible JR, Rougier GW, Novacek MJ, McKenna MC, Dashzeveg D. 1995. A mammalian petrosal from the Early Cretaceous of Mongolia: implications for the evolution of the ear region and mammaliamorph interrelationships. Am Mus Novit 3149:1–19.
Wible JR, Rougier GW, Novacek MJ, McKenna MC. 2001. Earliest eutherian ear region: a petrosal referred to *Prokennalestes* from the Early Cretaceous of Mongolia. Am Mus Novit 3322:1–44.
Wible JR, Novacek MJ, Rougier GW. 2004. New data on the skull and dentition in the Mongolian Late Cretaceous eutherian mammal *Zalambdalestes*. Bull Am Mus Nat Hist 281:1–144.
Wilson DE, Reeder DM, editors. 2005. Mammal species of the world. Baltimore, MD: Johns Hopkins University Press. 2 volumes, 142 p.
Witmer LM. 1995. The extant phylogenetic bracket and the importance of reconstructing soft tissues in fossils. In: Thomason JJ, editors. Functional morphology in vertebrate paleontology. New York: Cambridge University Press. p 19–33.
Zeller U. 1989a. Die Entwicklung und Morphologie des Schadels von *Ornithorhynchus anatinus* (Mammalia: Prototheria: Monotremata). Abh d senck naturf Ges 545:1–188.
Zeller U. 1989b. The braincase of *Ornithorhynchus*. Fortschr Zool 35:386–391.
Zilles K, Armstrong E, Moser KH, Schleicher A, Stephan H. 1989. Gyrification in the cerebral cortex of primates. Brain Behav Evol 34:143–150.